Tapio Tarvainen

Development of MorphHand: Exploring the design of soft robotics for upper limb prosthetics

School of Electrical Engineering

Thesis submitted for examination for the degree of Master of Science in Technology.

Espoo 7.4.2014

Thesis supervisor:

Prof. Raimo Sepponen

Thesis advisor:

Prof. Wenwei Yu

Aalto University
School of Electrical
Engineering

AALTO UNIVERSITY
SCHOOL OF ELECTRICAL ENGINEERING

ABSTRACT OF THE
MASTER'S THESIS

Author: Tapio Tarvainen

Title: Development of MorphHand:
Exploring the design of soft robotics
for upper limb prosthetics

Date: 7.4.2014 Language: English Number of pages: 7+58

Department of Electronics

Professorship: Applied electronics Code: S-66

Supervisor: Prof. Raimo Sepponen

Advisor: Prof. Wenwei Yu

This thesis describes the concept of a soft robotic hand prosthesis, namely MorphHand. It is developed to see, if the ideas of morphological computation and soft robotics could bring answers to some of the current problems in upper limb prosthetics.

The goal of the thesis was to explore the possibility of realizing the concept by 3D-printing the hand from rubber. This was done by manufacturing several soft one-piece finger prototypes, with compliant flexure joints. Their response was evaluated in bending tests, to see how changing different morphological parameters would affect their response.

The evaluated morphological parameters had the predicted effects on the prototype fingers' response, and the results showed that the proposed concept may be realizable. However, the used production methods should be reconsidered to make the fingers more durable and their response better.

Keywords: exploratory study, hand prosthetics, robotic hand design, two-joint prototype fingers, soft robotics, morphological computation

AALTO-YLIOPISTO
SÄHKÖTEKNIIKAN KORKEAKOULU

DIPLOMITYÖN
TIIVISTELMÄ

Tekijä: Tapio Tarvainen

Työn nimi: MorphHandin kehitystyö:
Tutkimusmatka yläraajaproteesien suunnitteluun
pehmeän robotiikan keinoin

Päivämäärä: 7.4.2014 Kieli: Englanti Sivumäärä: 7+58

Elektroniikan laitos

Professuuri: Sovellettu elektroniikka Koodi: S-66

Valvoja: Prof. Raimo Sepponen

Ohjaaja: Prof. Wenwei Yu

Tämä diplomityö kuvailee pehmeän robottikäsiproteesin konseptin, joka on nimetty MorphHand:ksi. Sitä kehitetään, jotta nähtäisiin voisiko morfologisen laskennan ja pehmeän robotiikan ideoita hyödyntää nykyaikaisia yläraajaproteeseja vaivaavien ongelmien ratkaisussa.

Diplomityön tavoitteena oli kokeilla voisiko tämän konseptin toteuttaa 3D-tulostamalla käden kumista. Tämä tehtiin valmistamalla useita pehmeitä prototyyppisormia, joissa oli joustavat, samasta rakenteesta tehdyt nivelet. Prototyyppien vastetta testattiin taivutuskokeissa, jotta nähtiin, miten erilaisten morfologisten parametrien muuttaminen vaikuttaisi siihen.

Testatut morfologiset parametrit vaikuttivat prototyyppien vasteeseen oletetuilla tavoilla ja tulokset osoittivat, että kuvailtu konsepti voi olla toteutettavissa. Käytettyjä valmistustapoja tulisi kuitenkin kehittää, jotta sormista saataisiin kestävämpiä ja niiden vasteesta parempi.

Avainsanat: eksploratorinen tutkimus, käsiproteesit, robottikäden suunnittelu, kaksinivelinen prototyyppisormi, pehmeä robotiikka, morfologinen laskenta

Preface

The idea for the thesis topic was born during my exchange studies in Chiba University, Japan, in 2011–2012. I was doing research in Professor Wenwei Yu's laboratory of Biointrumentation and Biomechanics, and also taking courses, such as the international ShanghAI Lectures. My interest towards prostheses, and the topics that were discussed in these lectures, transformed into an idea of a soft robotic hand prosthesis.

I was able to explore this concept of MorphHand, as I started to call it, because the laboratory had collaboration with a Japanese company, named Three Esu, or SSS, which specialized in 3D-printing. This led to printing rubber prototype fingers, based on a scan of my friend's index finger, and me writing this thesis about it.

As an ending for my exchange studies, I presented my preliminary results in the IEEE ROBIO conference, in December 2012, in China. This experience drove me to participate in the International Workshop on Soft Robotics and Morphological Computation, in Switzerland, in July 2013.

I am grateful to Aalto University and Chiba University for making my exchange studies possible, and The Finnish Society of Electronics Engineers (Elektroniikka-insinöörien seura ry) for providing partial funding for my exchange studies and workshop participation.

I wish to thank all the people, who have accompanied me and given their support in my journey. First of all, I would like to thank Professor Yu for taking me into his lab, making this research possible, and especially for his trust and patience as my advisor. My supervisor, Professor Sepponen, I thank for his open mind and supportive attitude towards my topic.

All the many friends I made in Japan deserve my gratitude for the good moments we had, especially Reijo for his stories and for lending a helping hand, and David, Jose, Nev, Yuan, Sekine, and everyone else from the lab for providing a pleasant working environment.

And finally, I wish to give my heartfelt thanks to my family for their unconditional support in this endeavor, especially my aunt Tiina for her academic expertize, and my fiancée Veva for her love.

I learned a lot about science, life, and especially myself during this long journey. Now, it is finally time to move on, and to find the next paths to follow.

Espoo, 31.3.2014

Tapio V. J. Tarvainen

Contents

Symbols and abbreviations

Abbreviations

Anatomy

CMC	carpometacarpal
DIP	distal interphalangeal
IP	interphalangeal
MCP	metacarpophalangeal
PIP	proximal interphalangeal

General

ADLs	activities of daily living
CNC	computer numerical control
DARPA	Defense Advanced Research Projects Agency
DoA	degree of actuation
DoF	degree of freedom
EB	Euler–Bernoulli (beam theory)
EMG	electromyography
EU	European Union
FEA	finite element analysis
HMI	human–machine interface
MPL	Modular Prosthetic Limb
PRBM	pseudo-rigid-body model
PWM	pulse-width modulation

1 Introduction

The recent advances in science and technology have enabled us to create upper limb prosthetics that were considered utopistic a few decades ago. Even controlling an external robotic hand through an implant placed in the brain has been successful [1]. But still, there is a long way to go before we can easily replace lost or defective body parts, even a non-vital one like the hand.

The current development points in hand prosthetics are related to comfort of use, costs, life-likeness of the device's appearance and function, and finally, the human–machine interface (HMI) and control, e.g. sensory feedback, and intention detection. Thus, there is still vast space for developing different prosthetic technologies further to get to the point of fully replacing a lost hand, or someday even augmenting it to enable a higher level of performance.

The traditional approach for tackling these challenges, has been designing a robotic hand with a complex kinematic structure, based on rigid mechanics. After this, a highly complex control system is developed around it to make it behave like a natural hand. The problem with this is, that we are trying to realize the function of a highly complex, soft, and nonlinear, biological structure, with a device that fits the engineer's mind and calculations. We need a lot of computational power, and a sophisticated interface, for controlling such a device to perform with the same finesse as the human hand. However, in a portable upper limb prosthesis, there is not enough room for such control systems.

Could it be, that as a rigid, structurally complex, and relatively easy to describe device seems to lead to a complex control, then vice versa, a soft and nonlinear, but structurally simple device would lead to a simple control? The idea, simply put, is transferring some of the control to the passive dynamic response of the device morphology, i.e. using morphological computation. Thus, the controller's limited computing power could be used more efficiently, while making the response of the device more natural. This is the logic the new field of soft robotics is using to approach the control problems, and to bring a different perspective on robotics.

The thesis considers the ideas of morphological computation and soft robotics, and takes an exploratory approach towards finding solutions for the issues in hand prosthetics. A soft robotic prosthetic hand, namely MorphHand, is developed on concept level, and several prototype fingers are designed and manufactured to test the concept, and a possible flow for producing it. This production flow includes scanning a real human hand's geometry, modifying it in CAD, and finally 3D-printing the fingers as functional monolithic (one-piece) rubber structures with embedded compliant joints.

After producing the prototypes, they are evaluated in bending tests to see the effect of different morphological parameters related to the compliant structure's geometry and material properties. Also an experimental air pocket structure around the joints is studied to see its possibilities as a functional and aesthetic supporting structure.

The thesis starts with a background on the theory and ideas behind the concept of MorphHand, the soft robotic hand prosthesis. This consists of a literature re-

view on the human hand, in Chapter 2, upper limb prosthetics, in Chapter 3, and theory related to morphological computation and soft robotics, in Chapter 4. The review acts as a basis for defining the concept of MorphHand and its requirements, in Chapter 5. Next, Chapter 6 describes the process of developing the finger prototypes, and the methods that were used to study their response. The results of the experiments are presented in Chapter 7, and discussed in Chapter 8. Finally, Chapter 9 concludes the work.

2 Human hand

We use our hands to interact with the world and to communicate. They enable us to do a wide variety of tasks, ranging from robust handling of large objects (e.g. displacing a large stone) to fine manipulation of small tools (e.g. sewing). All this is possible through their complex biological structure, which makes them inherently soft and adaptive. The human hand is a remarkable example of how versatile mechanisms the natural evolution can create [2,3].

This chapter describes the human hand and the aspects that enable its inherent versatile dexterity and adaptiveness. The goal is to provide the essentials for understanding the function of the hand in the context of designing a hand prosthesis. First, Section 2.1 gives a short introduction to the morphology, i.e. the anatomy, of the human hand. Then, Section 2.2 goes through its inherent movement capabilities, i.e. its kinesiology. And finally, Section 2.3 describes its development and function.

2.1 Morphology

The human hand consists of 27 bones, excluding the forearm radius and ulna, and the variably occurring sesamoid bones. The bones of the hand are shown in Fig. 1(a). The wrist has eight bones, called the carpals, that connect the hand to the radius and ulna in the forearm. Five metacarpal bones, connected to the carpals, form the palm and the base of the thumb. Finally, the digits are made up of phalanges, proximal, medial, and distal, with the thumb having only proximal and distal [2–4].

The movements of the hand are enabled by joints that connect the bones, allowing their heads to roll and glide fluently against each other. The ellipsoid joints that connect the digits to the palm are called metacarpophalangeal (MCP) joints and the hinge joints joining the phalanges are called interphalangeal (IP) joints. In the fingers, the two interphalangeal joints are distinguished as proximal (PIP) and distal (DIP). The thumb has a saddle joint in its base, called the carpometacarpal (CMC) joint, which enables its wide range of movement. Finally, the wrist joint consists of several articulations between the radius, ulna, carpals, and the metacarpals. For simplicity, here this complex structure is referred to only as the wrist, or the wrist joint [2–4].

Over the skeleton there are soft tissues. They enable and restrict the movements of the hand, provide its sensory functions, take care of its metabolism, and protect it by lubricating the moving parts, fixing unavoidable damage over time, and adapting to changing external conditions, such as temperature shifts and recurring abrasive forces. These soft tissues include muscles, blood vessels, nerves, fat, skin, and connective tissues, such as ligaments that connect the bones and cover the joints, tendons that attach the muscles to the bones, and fibrous sheaths that protect and guide the tendons [2–4].

There are approximately 36 muscles that actuate the movements of the hand. The exact amount varies between individuals, some having multiples and others missing some of them completely. The muscles are divided into extrinsic, located in the forearm, and intrinsic, within the hand. The extrinsic muscles actuate the

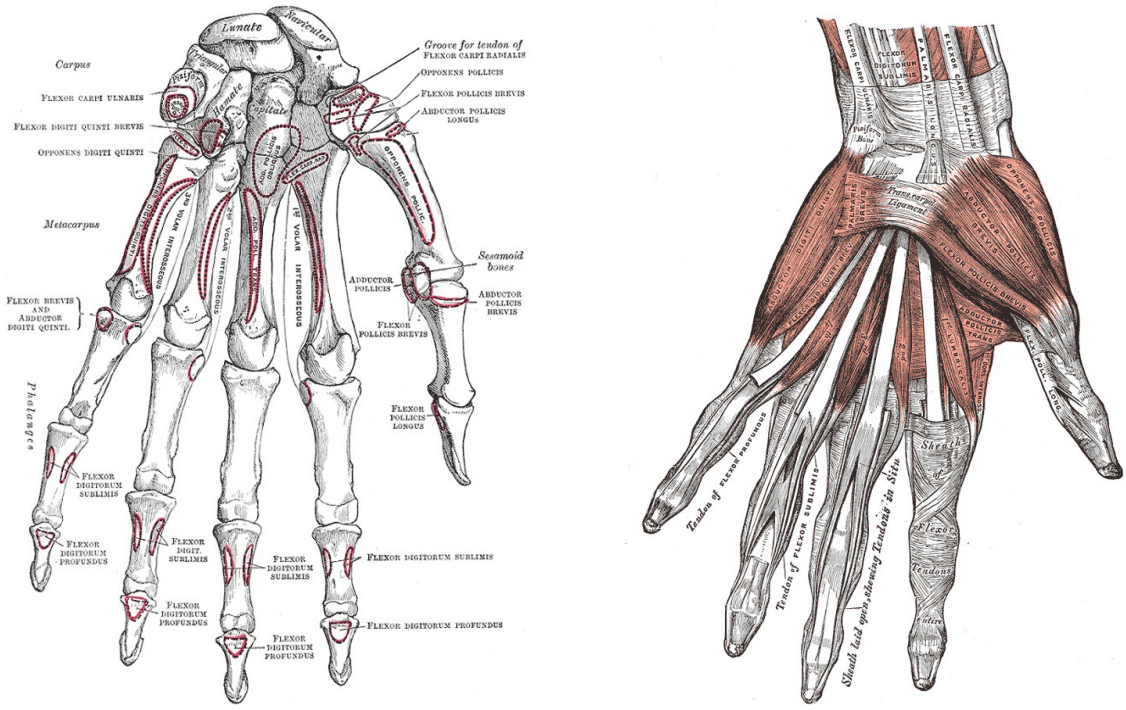

(a) Bones. Tendon connections indicated in red.

(b) Muscles and fibrous tissues.

Figure 1: Structures of the left hand, palmar view [4].

wrist, the fingers' flexion and extension, and some of the thumb motion. The precision movements, such as the sideways movement of the fingers, and most of the movements of the thumb, are done by 18 small, intrinsic muscles [2–4].

Contractions of the muscles are intermediated to the skeleton by a complex, interconnected network of tendons that are guided and protected by tendon sheaths around them. The complexity and connections restrict some of the movement, but also make the network redundant. If there is damage to one part, there is usually another to replace it. This way, although some fine manipulation skills may be lost, the basic functions are usually maintained [2–4].

The hand's sensory system, and the muscles that actuate it, are innervated by three nerve branches, radial, median, and ulnar that travel under the shoulder to the arm. The radial nerve innervates all the extensors of the elbow, the wrist, and the fingers. It also innervates a major part of the skin over the back of the hand. Next, the median nerve is the most important sensory nerve. It innervates most of the palmar skin, and most of the skin over the first three and a half digits. It innervates the extrinsic flexor muscles of the wrist and the digits, and also some of the intrinsic hand muscles. And finally, the ulnar nerve innervates two flexor muscles and most of the intrinsic hand muscles. It also innervates the rest of the skin on the little finger's side of the hand [2–4].

In the end, everything from the wrist to fingertips adds up to approximately 0.5 % for adult women, and 0.6 % for adult men, of the full body mass. For an

average man weighing 80 kg this would mean 480 g. Here, it is also relevant to consider how much the forearm weighs, because it contains the major muscles for hand actuation. In relation to the whole body mass, the weight of the forearm is approximately 1.3 % and 1.7 % for women and men, respectively. Relating this to the example 80 kg male, it would mean 1.36 kg, or 1.84 kg, when including both the hand and forearm [5].

2.2 Kinesiology

The joints of the hand give it at least 27 degrees of freedom (DoFs). Each digit, including the thumb, has 4 DoFs. The palm has 1–2 DoFs, from the movement of the 4th and 5th metacarpal bones, which brings the little and ring fingers closer to the thumb. This, and the wide movement range of the thumb, enable opposition of the thumb and fingers, a rare ability in the animal kingdom. Finally, the wrist has 6 DoFs, three of them being the flexion/extension, pronation/supination (i.e. the rotation of forearm radius and ulna relative to each other in thumb direction and the opposite, respectively), and radial/ulnar deviation (i.e. sideways movement in thumb direction and the opposite, respectively). The other three DoFs come from the less distinctive translation and rotation of the wrist bones [2–4, 6, 7].

Each joint has its range of motion defined by its structure, the surrounding soft and connective tissues, and the tendons that connect the bones to the muscles. Table 1 shows the different maximum flexion and extension angles for each digit. These angles vary greatly between individuals, comparing, for example, the thick fingers of a carpenter to those of an office worker. Many times the difference can be around $\pm$ 10°. Furthermore, the results depend strongly on the chosen measurement method, whether one uses motion capture with markers attached to the finger, or determines the angles from x-ray images, etc. [2, 3, 8–10].

The complex structure of the actuation of the hand affects the force distribution and moment arms during grasping tasks. This positions the bones and tendons to better accommodate the forces in different grasps, and causes the free flexion of the fingers to have a certain sequence. The flexion begins normally at the level of the PIP joint, followed by the MCP and DIP joints. The DIP joint flexes slower than the PIP joint, and its flexion is completed only at the end of the movement, locking the grip. Furthermore, the extension starts at the level of the MCP joint, followed by the PIP and DIP joints. This flexion-extension sequence contributes to the natural adaptiveness of human grasping. Upsetting it, e.g. due to partial neural paralysis, causes strong impairment of the grip [3, 11].

Another property of the upper limb, is its compliance, which varies depending on the task. It can be stiff, when bracing oneself against an expected blow, or relaxed, when playing the piano. This inherent compliance provides protection for the joints and musculoskeletal system, so that they can withstand external shock loads far better than a rigid, stiff-jointed equivalent [7].

The next section describes how the hand's morphology and kinesiology contribute to its inherent flexible function as a manipulator.

Table 1: Average maximum flexion and extension angles for the phalangeal joints of each digit, combined from measurement data by Barakat et al. [8] and Leijnse et al. [9].

Digit	Joint	Average maximum flexion (deg)	Average maximum extension (deg)
Thumb	MCP	60 ± 6	8 ± 4
	IP	88 ± 2	12 ± 9
Index	MCP*	102 ± 11	61 ± 24
	PIP	115 ± 4	20 ± 11
	DIP	80 ± 9	32 ± 11
Middle	MCP*	102 ± 11	61 ± 24
	PIP	117 ± 5	21 ± 15
	DIP	91 ± 7	26 ± 11
Ring	MCP*	102 ± 11	61 ± 24
	PIP	119 ± 6	19 ± 13
	DIP	86 ± 10	25 ± 18
Little	MCP*	102 ± 11	61 ± 24
	PIP	110 ± 7	11 ± 12
	DIP	90 ± 11	42 ± 22

*Average of 2nd to 5th digits' MCP joints.

2.3 Development and function

Our central nervous system controls our limbs by sending commands to the muscles, consciously and through reflexes, and by getting feedback from the sensory system. This exchange of information, combined with the previously described morphology, enables the high level of control and dexterity we can observe in manipulation tasks. Proprioception, i.e. the inner conception of ones body position, plays an important role here. It allows us to sense, with vision blocked, the position, and active and passive movement of our arms and hands. It works in unison with visual feedback, when we perform tasks, such as reaching and grasping [2, 3].

Our dexterous manipulation skills change and develop throughout our lifetime. This happens especially during childhood, as our body grows, and our sensory systems and neural connections develop, while we learn to interact with the world. By the age of 18, the length and width of our hands have grown by a factor of 200–300 %, and we have mostly gained the adult level of sensing and dexterity. Along the way, our body adapts to our way of living, and we adopt new ways of using our hands. Some we learn automatically, through the activities of daily living (ADLs), such as eating, dressing, and managing personal hygiene. Some come only through rigorous training, e.g. skills in martial arts. As we grow older, the acquired skills adapt to the changes in physiology that come with age. We lose strength, and our

movements become slower due to muscle mass reduction and as the slow muscles become prevalent. Also, our skin gets thinner and dryer, causing loss of friction in our grip [2].

The manual skills can be divided into prehensile and non-prehensile. Prehensile meaning the manipulation of objects by grasping them with our fingers or hands, e.g. holding a pen to write notes. Non-prehensile, on the other hand, meaning the skills that do not involve having complete control of the manipulated object, e.g. holding a book on the palm of the hand. Also, non-prehensile tasks do not always involve an object, e.g. gesturing while communicating. The skills can be further divided into subgroups of power and precision, based on their finesse, stability, and contact area, e.g. enveloping a pen in the hand vs. holding it with the fingertips, or pushing a boulder with the whole hand vs. typing on a keyboard. These are then divided into subgroups depending on the size of the manipulated object, and the number and combination of used digits for the task [2, 3, 7].

In bimanual manipulation we use our both hands to take full advantage of their abilities. The second manipulator provides more contact to large objects, and makes it easier to explore the shape, symmetry, size, and contours of the environment. It makes manipulation easier by providing more degrees of freedom, and two separate fixing points for the objects. If one hand is lost, a major part of manipulation abilities is lost, and the other is left in an almost sterile isolation [2, 3].

In a manipulation task, the required forces and speeds depend on the weight, size, and state of the grasped object, and the type of grasp. The human hand is capable of speeds in excess of 40 rad/s (2290 deg/s), and grasp forces up to about 400 N. Everyday pick-and-place tasks have average speeds in the range of 3 to 4 rad/s (172 to 200 deg/s), while most ADLs require grasp forces in the range of 0 to 67 N. There is also a force difference between the fingers. The middle finger is the strongest (33.5 % of overall force of the four fingers), then the index and ring fingers (25 %), and finally the little finger (16.5 %) [2, 3, 7].

The inherent properties of the skin reduce the required forces for holding an object. This makes its manipulation easy and energy efficient. Softness of the hand makes it adapt to the shape of the object, thus maximizing the contact area. This natural softness of the palmar skin is enabled by its maintenance system that keeps it constantly hydrated. Also, the uneven contours of the skin contribute to maximizing the friction between the hand and the object [2, 3, 7, 12].

Having this valuable tool of interaction disabled, or losing it completely, affects an individual's life dramatically. Even losing a single digit may have a major effect. Approximately 40 % of the whole hand's function is lost when the thumb is removed. For the others digits, from index to little, the respective values are 20 %, 20 %, 10 %, and 10 % [2].

The next chapter takes a look at the current state of the art technologies we have for replacing a lost or disabled hand.

3 Hand prosthetics overview

Until the mid 20th century, all prostheses were passive, or mechanical and body-powered. The turning point came around 1949, when the first working model of an electrically powered artificial arm was developed. Later, in 1958, the first myoelectric hand prosthesis was developed in the USSR. Since then, the technological advancements in robotics, electronics, material science, bioengineering, medicine, etc., have given us the tools to develop increasingly advanced and complex robotic manipulators for use in prosthetics [13, 14]

This chapter gives an overview on hand prosthetics and their development, by listing their requirements and current problems, and by describing the state of the art. First, Section 3.1 reviews the requirements for upper limb prostheses. Then, Section 3.2 takes a look at the current state of the art research and commercial myoelectric prostheses, giving their essential specifications that affect their function. And finally, Section 3.3, goes through the current design priorities in upper limb prosthetics.

3.1 Requirements

Whenever a prosthesis is needed, an integral part of the body has been lost. The goal is to replace it, so that the person could continue living preferably in the same manner as before. This means that the prosthesis should become a new integral part of the amputees body, replacing the original limb, and bringing back the functions that were lost. Intuitively, this would be easiest to achieve by creating a device that is as similar as possible to the original, ideally grown from the same biological material, and surgically connected back to its place. But, as long as we are not able to grow back limbs, we need to improvise with the technology we have, to make devices that bring back most of the lost function, and are also comfortable to use.

To do this, we need to consider the many aspects of designing a prosthesis. These are related to the patient's individual needs and requirements, mechanical and functional requirements for the device, and finally, the HMI and control. Here, we will go through these different design considerations, starting from the patient's needs.

Patient's needs

All amputees have their individual needs for the prosthesis. These needs are based on personal preferences, the cause and level of amputation, and the shape and size of their body. Thus, it is difficult to develop a single prosthesis that works for everyone. This is why prosthetics manufacturers usually offer different models that are based on average body sizes, and answer to different desires related to functionality and cosmesis [7, 15].

Saito et al. [15] pointed out that the most favorable prosthetic hands to the patients, both in size and appearance, are those that fit their age and body shape. Particularly for those who have a remaining real hand, it is important for the prosthesis to match its shape and size. Take, for example, a hand prosthesis that is

designed in Germany, based on statistical average body sizes in Europe. A German male amputee might find it quite suitable, while a Japanese female would consider it literally humongous. Even a version designed for females might seem large, and more of the size of an average male hand in Japan [15].

The correct size and shape are part of the aesthetics and cosmesis of the prosthesis. Aesthetics refers to the effect of the device's appearance and function, on the patient's subjective perception of it. Cosmesis, on the other hand, refers to the ability of the device to mimic the appearance, i.e. the looks and movement, of a real hand. Both are important in making the amputee feel comfortable using the prosthesis, and accept it as an extension of their body. However, the requirements for cosmesis depend a lot on the amputee's individual preference. Some may be very concerned about it, and may sacrifice functionality by choosing the more natural looks of a passive prosthesis. Some, on the other hand, enjoy the robotic appearance, and are more concerned about functionality and the overall aesthetics of the device. It is also common to have two prostheses, one functional for work, and another cosmetic for social occasions [7, 16, 17].

Also the costs associated with acquiring a prosthetic device and taking care of its maintenance are important for the amputees, especially in lower income classes and developing countries. The initial costs include the price of the device and connecting components, and the payment for the work done by prosthetists and other medical professionals, when fitting the prosthesis. The recurrent costs include device maintenance and repair, and the price of the consumable spare parts, such as cosmetic gloves. These costs may become especially high when a child needs a prosthesis. The growth of the patient requires almost annual adjustment of the shape and size of the device, which usually means replacing the prosthesis with a new one. This increases the financial burden on the family, especially if a highly functional device is used, because they tend to have a price range from thousands to several tens of thousands euros [15, 18–20].

Mechanism and function

The patient's needs, and the function and features of the real human hand, set the goals for prosthetics development, e.g. cosmesis, level of functionality, and comfort of use. However, the available technologies, such as materials, and suitable actuators, set the limits to what can be achieved.

First of all, the weight of the human hand gives a clear limit to how much the replacing device, with all its components, can weigh. Although the adult hand weighs approximately 300 to 550 g, a prosthetic hand should always weigh less, because it is not connected directly to the skeleton. The primary way of connecting a hand-arm prosthesis is through a socket that grips tightly around the stump. Thus, the soft tissues have to mediate the load to the skeleton. This causes the patient to feel that the prosthesis is heavy, even though it may have the same weight as the original limb. It may be possible to increase this weight limit in the future, by using osseointegration, where the prosthesis is attached to a titanium implant that protrudes through the skin [7, 18, 21].

In addition to the weight limit, the size and shape of the human hand define how much space there is to accommodate the required components of the prosthetic mechanism. This effectively restricts the amount and size of the used components, actuators, power sources, and control circuits. And these, in turn, limit the hand's possible functions [7].

The physical constraints make the attempt of making a fully functional anthropomorphic prosthesis extremely difficult and expensive. Furthermore, certain tasks, such as carrying a bag, or holding a spoon when eating, may be easier and more effective to accomplish with a much simpler device, such as a standard hook prosthesis. This suggests that anthropomorphic solutions may not be optimal due to their complexity. However, as Bicchi [22] and Ma et al. [23] state, in prosthetics, where aesthetics and similarity to the original hand are a concern, it may be considered justified to aim for similar dexterity and redundancy [7, 22, 23].

Based on a multidisciplinary study by Peerdeman et al. [24], the main grasp types that should be possible with a functional prosthetic hand, are lateral, cylindrical, and tripod grasp. Also, index finger pointing is mentioned as an important gesture for various other activities, such as typing on a keyboard. Furthermore, wrist movements, especially rotation and flexion/extension are important in avoiding awkward elbow and shoulder motions in positioning the hand for grasps in a natural manner. In a hand-like prosthesis, it takes approximately six independently controlled DoFs to achieve all these movement patterns [7, 24].

The actuation of the prosthesis should also be fast enough, so that the user does not get disturbed by the execution time. Moreover, the hand should provide enough grasping power to hold both light and heavy objects, and be able to adjust it for manipulating different objects with different weights, for example when carrying a bag, or holding an egg [7, 15, 24].

Human–machine interface and control

By designing the mechanism correctly, we can get a machine that has the potential of performing complex functions, similar to those of the natural hand, while still keeping it in the required weight and size limits. But to bring out this potential, we need to control the device through an interface between the amputee and the machine. In modern functional prostheses this is either done through movements of the body via a harnesses, or through a myoelectric interface, with usually one of two electrodes on the amputee's stump, that record the electromyographic (EMG) signals generated by the remaining muscles. In body-powered devices, a control designer needs a wide knowledge on the human movement ranges that could be utilized. In myoelectic ones, the focus is on designing a control circuit that analyzes the recorded EMG waveform, and makes control decisions accordingly [7].

As Weir and Sensinger [7] point out, controlling a prosthetic limb can be compared to operating an excavator that has multiple DoFs. The driver needs to focus on the task constantly and use all limbs for pulling levers and pressing pedals. The amputee should be able to do all this through a much simpler interface, without it affecting their other functions. In this case, a two-electrode EMG interface could be

compared to having only a pair of buttons to press, when operating the excavator. Implementing a HMI and a controller that achieve a high level of function, with minimal mental burden, is currently perhaps the most difficult problem to solve in functional anthropomorphic prostheses [7].

Childress listed the requirements for hand prosthesis control in 1992 in the following form (as cited by Weir and Sensinger, 2009) [7]:

1. **Low mental loading or subconscious control:** It should be possible to use the prosthesis without undue mental involvement. The prosthesis should serve the user and not vice versa.

2. **User-friendly or simple to learn:** Any device should be intuitive and natural. An amputee should be able to learn to use the prosthesis quickly and easily.

3. **Independent control of multiple functions:** Control of any function or DoF should be possible to execute without interfering with the other control functions of a multifunctional prosthesis.

4. **Simultaneous, coordinated control of multiple functions:** The ability to coordinate multiple functions simultaneously, in effective and meaningful ways, without violating the first and third attributes.

5. **Direct access and instantaneous response:** All functions, if possible, should be directly accessible to the user, and these functions should respond immediately to input commands.

6. **No sacrifice of human functional ability:** The prosthesis should be used to supplement, not subtract, from available function. The control system should not encumber any natural movement that an amputee can apply to useful purposes.

7. **Natural appearance:** Movements that appear mechanical in nature, attract unwanted attention in social situations, and may not be pleasing to the eye.

Almost twenty years later, in 2011, Peerdeman et al. [24] gave a similar, but a more specified list, based on the current technologies. The list, shown in Table 2, describes the requirements for the EMG interface, control, and feedback. It is easy to see that the main requirements have not changed since the beginning of the 1990s [24].

Especially the ability of easily performing the main grasps and wrist movements, with minimal time delays, was seen important. The prosthesis should also automatically continue holding a grasped object, and prevent it from slipping. Also force and position feedback were defined crucial. These are important in manipulating fragile objects, such as eggs, interacting with humans and other animals, and allowing for intuitive grasping. Without feedback, the applied force, and the current posture of the hand have to be determined only through visual inspection, which increases mental burden [24].

Table 2: Functional requirements for myoelectric prostheses' interface and control, categorized by subsystem, and in the order of importance, adopted from the listing by Peerdeman et al., in 2011 [24].

Subsystem	Requirement
EMG interface	1. Multiple easily selectable wrist movements and grasps
	2. Nondisturbing time delays
	3. Proportional control of force and speed
	4. Simultaneous control of wrist movements and grasps
Control	1. Grasp types: cylindrical grasp, tripod grasp, lateral grasp
	2. Wrist movements: flexion/extension and rotation
	3. Automatic holding of grasped object
	4. Automatic slip prevention
	5. Reasonable grasp execution times
	6. User controlled force and speed
Feedback	1. Grasp force feedback, continuous and proportional
	2. Position feedback
	3. Easy and intuitive
	4. Discreet
	5. Adjustable

3.2 State of the art prosthetic hands

This section describes the state of the art in upper limb prosthetics. Therefore it concentrates on the newest multi-DoF electromechanical prostheses, and excludes single-DoF electromechanical, body-powered, and passive hands.

We will first take a look at the Modular Prosthetic Limb (MPL), which is currently the most advanced existing upper limb prosthesis, to see the level that has been reached in research. Then, we will move on to the most advanced commercially available myoelectric hands, which are beBionic3 from RSLSteeper, i-Limb Ultra Revolution from Touch Bionics, and Michelangelo from Otto Bock.

All these hands have several DoFs, and are capable of executing different grasp patterns based on the user's input. While the MPL uses experimental and expensive HMIs, all the commercial hands have to settle for a one or two-electrode myoelectric HMI for control. This EMG control is based on preprogrammed movement sequences that the user chooses with a series of predefined muscle contractions. Furthermore, working sensory feedback has only been realized in research setting, and in all the commercial hands, the only feedback for the user is visual [1, 17, 25–33]

A recent development in commercial prostheses, has been the availability of increasingly life-like cosmetic gloves. Especially Touch Bionics and RSLSteeper, being dependent on their flagship prosthetic hands, have developed these technologies. Besides taking the patient's skin color into account, they are also adding nail structures, and even hair to the gloves [28–31]

In the following, we will go through the main specifications of each of these four state of the art electromechanical prostheses. Further details on the current myoelectric prostheses, and their performance, can be found for example in the reviews done by Belter et al. [34, 35].

MPL, DARPA

Currently, the most advanced prosthetic hand could be considered to be the Modular Prosthetic Limb (MPL), which is developed in a project sponsored by the U.S. Defense Advanced Research Projects Agency (DARPA). It represents the traditional approach at its finest, but is still a research device, and thus extremely expensive [1, 25, 26].

The complete prosthesis has 26 DoFs in total, with 21 degrees of actuation (DoAs). The arm has 4 DoFs/DoAs, the wrist 3 DoFs/DoAs, and the hand 15 DoFs and 19 DoAs, with a fully actuated 4 DoF thumb. The hand is actuated by intrinsic electric motors. Based on the given details, the hand should be able to achieve almost all the same functions as a real one. Furthermore, direct control and sensory feedback through neural interfaces and brain implants have been tested [1, 25, 26].

As the MPL is a research device, some of the details, such as its actual weight or size have not been disclosed. However, based on the stated requirements, the complete prosthesis should weigh approximately the same as an average human upper limb, and have approximately the same dimensions [25, 26].

beBionic, RSLSteeper

RSLSteeper is an England-based company providing prosthetics, orthotics, and other assistive technologies and services. Their main myoelectric upper limb prosthesis is the beBionic hand, currently in its third version, beBionic3 [27, 28].

It has overall 12 DoFs: 2 DoFs for each finger, 3 DoFs for thumb, and 1 DoF for wrist rotation. The thumb is positioned manually between the opposition and lateral positions. Fingers' sideways movement is incorporated into flexion/extension by having them close to each other in flexion, and separating them in extension [27–29].

The hand's 12 DoF structure, the adaptive finger flexion, and wide programmability enable all the main grasp types and gestures, and also specialized grasps. For

example, there is a ready function for holding a computer mouse with the thumb and little finger, while clicking it with the index finger. The 2 DoF fingers also adapt to some degree to the shape of the grasped object by stopping the joints that experience resistance, while the free joints continue to the programmed final posture [27–29].

The beBionic3 is offered in medium and large sizes, with three different wrist types. Weight of the hand, without a cosmetic glove, ranges from 570 to 698 g, depending on the chosen configuration [27–29].

i-Limb, Touch Bionics

Touch Bionics is a Scotland-based company, specialized in active and passive upper limb prostheses. Their main myoelectric hand prosthesis is called the i-Limb. Its newest version being the i-Limb Ultra Revolution [30].

The hand has overall 10–13 DoFs: 2 DoFs for each finger, 2 DoFs for the thumb, and 0–3 DoFs for the wrist. The thumb opposition is fully actuated. The wrist has several configuration options, with a possibility to add a wrist rotator, or manual positioning in sideways or flexion/extension direction [17,30,31].

Possible grasps include the main grasp types from power grasp to precision pinches, gestures, and special grasps. As with the beBionic3 hand, i-Limb's fingers adapt to the shape of the grasped object by continuing the joint movement until they experience resistance, or reach the final position in the current grasp's execution. There is also a mobile application for controlling the hand, choosing the active postures, and training. [17,30,31].

The i-Limb Ultra Revolution is offered in medium and small sizes, with three different options for the wrist. The weight varies in the range of 443 to 515 g, without the prosthetic glove, depending on the chosen wrist type [31].

Michelangelo, Otto Bock Healthcare GmbH

The German prosthetics company Otto Bock offers a wide variety of disability related products, including several robotic hand prostheses, also for children. Their current flagship product is the Michelangelo hand, which is promised to have a natural appearance and function through its use of soft materials and a complex kinematic structure [32,33].

Michelangelo has overall 5 DoFs: 1 DoF for the fingers, 2 DoFs for the thumb, and 2 DoFs for the wrist. The fingers have only one joint and move always in unison. Their sideways movement is incorporated into flexion/extension as in beBionic3. The thumb movements are fully actuated. Also wrist flexion/extension is actuated, but wrist rotation is done manually, 360° in both directions. The wrist flexion/extension has two modes, rigid and flexible. In the flexible mode the wrist is said to imitate natural wrist behavior, while in rigid mode it is locked in place when not actuated [33].

The hand structure enables power grasp with thumb in opposition or lateral position, tripod and lateral pinch, and suitable wrist positioning. However, basic finger gestures, such as pointing with the index finger are not possible [33].

The Michelangelo is offered in one size (M), and it weighs approximately 420 g without, and 498 g with a protective glove [33, 35].

3.3 Current design priorities

In 2007, Biddiss et al. made a wide, 200 article review on upper limb prosthesis use and abandonment covering the previous 25 years [36], conducted an anonymous internet survey on design priorities in upper limb prosthetics [18], and described the critical factors for device abandonment [19]. These studies showed the main reasons for the amputees abandoning the use of a prosthesis and choosing another, or even deciding to live without one. They also provided guidelines and directions for future research [18, 19, 36].

Physical comfort of use

Comfort of use and device weight were the most important factors in prosthesis abandonment. The issues are mostly related to the user–device connection, which often defines whether a patient will wear the prosthesis or not [7, 18, 19]

The commonly used sockets tend to be hot and uncomfortable to wear for long periods of time, because they envelop the stump and cause abrasion in the soft tissues. Especially electromechanical prostheses with their motors and batteries generate excess heat that accumulates in the socket. These issues cause discomfort, fatigue, and medical problems, such as skin irritation and blisters [7, 18, 19].

The comfort and weight issues call for continued exploration of light-weight materials, improved heat dissipation, and alternative socket designs or connection techniques (e.g. osseointegration) [7, 18, 21].

Functionality, HMI, and control

Functionality took the second place as a cause for rejection. Most amputees that had rejected the use of a prosthesis completely, told that they had just as much, or even more function without it. The reasons for this were the lack of sensory feedback, difficulties in use and training, and restricted joint movement ranges that did not enable good enough dexterity for fine motor skills [18, 19, 36].

The need for better functionality reflects to the design of the mechanism, its control, and the user interface. This justifies the ongoing research in finding practical, non-distracting sensory feedback methods, developing the interfaces, and inventing more dexterous hand mechanisms [18, 19, 36].

Appearance

Appearance has become more and more important, also in active prostheses. Amputees seem to be increasingly unwilling to make trade-offs between function and appearance, and want both in the same device. The demand for a more natural, life-like appearance, increases the requirements for commercial prostheses that are traditionally made to be either cosmetic or functional [18, 19, 36].

While the recent development of more and more life-like cosmetic silicone gloves have improved the passive appearance of the prostheses, there is still a lot of room for improvement in making also the actuated appearance natural [7, 18, 19, 36].

Durability and cost

Although cost was not ranked high in the survey by Biddiss et al. [18], it is an area where improvements are desired. This is especially the case for patients, whose insurance or medical coverage is limited. Also the durability of the device, and especially the protective/cosmetic glove, remain a concern. The modern multi-DoF hands tend to be less robust than simple hooks, and the gloves have problems particularly with regard to staining and discoloration. The high price of the modern multi-DoF hands and their life-like gloves, make this even more important [18,19,36].

This leads to the need for more robust mechanisms and better, cheaper materials. A demand for low-cost, durable prosthetic solutions may also lead to the development of more suitable devices for developing nations, where these design concerns are especially important [18, 19]

4 Morphological computation and soft robotics

This chapter describes the new fields of morphological computation and soft robotics, and the fundamental ideas behind the concept of MorphHand. It also describes the used terminology in their context.

The chapter starts by explaining the theory of morphological computation, and then moves on to showing its application in the field of soft robotics. After this, it presents some examples of soft robotic hand projects, and finally gives some details on how these soft systems are designed and analyzed.

4.1 Computation through morphology

The basic idea behind morphological computation is that all behavior of an agent emerges from the interaction between its morphology (body), and its control (brain), and/or environment. A simple illustration of this relation is shown in Fig. 2. The agent in this case can be a human, another animal, or any other thing, e.g. a robot, that interacts with its environment through its morphology. Morphology is defined as the physical structures within the agent, including its sensors [37–42].

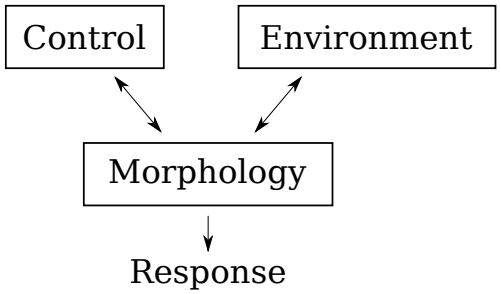

Figure 2: The interaction between an agent's morphology (body), and its control (brain) and/or environment results in a response (behavior) defined by its morphological properties.

Morphological computation in itself means that certain processes are performed by the morphology that otherwise would have to be performed by the control. In other words, it is the ability of a physical system to accomplish control functions, or computing, by taking an input and producing an output. This means that some of the control is embodied in the system's morphology. When applying this principle in design, the goal is to transfer some of the control from the controller to the active and passive response, or passive dynamics, of the structure [39–41].

An example of morphological computation that emerges from body–brain interaction, is the human hand and wrist. When you flex and extend your wrist, and keep your hand otherwise passive, the fingers extend and flex automatically with the movement. The finger movement happens through the hand's complex morphology, and control is only applied to the wrist movement. We unconsciously take advantage of these inherent movements of our body all the time in our everyday life, for example when picking up objects [39].

A classic non-biological example of morphological computation in body–environment interaction, is the passive dynamic walker (PDW). A PDW is a, usually bipedal, completely mechanical structure that has no controller at all. Thus, all the behavior that the PDW exhibits, emerges from the interaction between its morphology and the environment. This is also referred to as passive dynamics. The basic PDW, which has no internal power source, can walk fluently down specific slopes with the potential energy it gets from gravity. However, when the slope ends, or it is not favorable, the PDW falls down. This shows that with a certain morphology, and with certain environmental constraints, the device can exhibit a complex, or intelligent, response. However, it does not have a brain, which is traditionally thought of as the source of such behavior [39, 43].

In 2006, Paul [40] considered the use of morphological computation for transferring control from a robot's controller to its morphology, and thus reducing the control requirements. She examined different cases of robot morphology, and came to a conclusion that this kind of transfer is indeed possible, if the robot has a high level of dynamic coupling in its structure. In 2011, Hauser et al. [38] got similar results, by simulating nonlinear mass-spring systems. They showed that these systems could be used for emulating arbitrary, time-invariant, nonlinear filters with fading memory. Their conclusion was, that morphological systems can be computationally powerful, if they are parametrically complex and high-dimensional, as in biology. However, these properties make quantitative analysis of the system extremely complex, and are thus avoided in traditional robot design [38, 40].

In hand prosthetics, morphological computation could be used, for example, for solving issues in EMG control. Because of the restricted amount of electrodes, and noisiness of the signal, the EMG interface is difficult to use for exact control of the hand. If some of the control of the prosthesis would be transferred from its controller to its morphology, its use could be made simpler, more natural, and intuitive. This could be done for example by using soft, compliant materials, and underactuation, i.e. by having more DoFs than actuators. Then the hand would adapt to the shape of a grasped object, maximizing the contact area, and making the grip more stable. This would reduce the required force and the requirements for control [38, 40, 41].

The next section discusses the application of morphological computation in the field of soft robotics.

4.2 Softness and compliance in robotics

The new field of soft robotics is, in essence, an application of morphological computation. However, the goals in different soft robotics projects range from exploring natural phenomena in biological systems, and studying artificial intelligence, to developing more efficient manipulators for industrial applications. Whatever the final goal, the main idea is always to use softness, or in other words, high level of nonlinear compliance, as the key element in designing and studying these robots. The point in this, is to gain similar features that are inherent in biological systems, such as flexibility in movements, fluent operation in non-structured environments, and robustness against sudden forces through compliance. In the end, besides creating

more efficient artificial systems, we learn a lot about how the nature works [44–46].

An example of recent soft robotics research, is the OCTOPUS Integrating Project funded by the EU's 7th Framework Programme. The goal of the project is to analyze and understand the mechanisms that enable the versatile sensory-motor capabilities of the octopus. This is done through creating an eight-legged biomimetic soft robot that has equivalent abilities in an underwater environment. So far, only separate, soft tentacle manipulators connected to a rigid body have been made, but a massive amount of scientific publications, on topics related to morphological computation, and soft, biomimetic robots, have been generated around them [44, 45, 47].

Another relatively famous example project is the starfish-shaped quadruped robot, which was originally developed by the Whitesides Group, in Harvard University. It is composed of a silicone body with five embedded pneumatic actuators. The bottom of the robot is made of a nonextensible layer, which causes the structure to bend, when the actuators are pressurized. This way it can perform different kinds of gaits, or movement patterns, and adapt to the shape of an object, when grasping it [48].

These examples show that the field is still forming through different imaginative projects, and it is finding its way into practical applications, while searching for its place in the global scientific community [44, 46]

The following sections will continue, by giving some examples of soft robotic hands, and describing different methods that are used to design and analyze these complex, soft systems.

4.3 Soft robotic hands

This section describes a selection of recent projects on soft robotic hands. It tells shortly about their goals, and gives essential details on the developed hand structures. The projects are introduced in the order of applied compliance, starting from the most rigid and ending in the softest one.

UB Hands III and IV, and the DEXMART Project

A series of robotic hands have been designed in the University of Bologna's UB Hand projects. The latest of them is UB Hand IV (or DEXMART Hand), which was developed in the DEXMART Project, funded by the European Union's (EU) 7th Framework Programme. The goal of the DEXMART Project was to study novel robotic technologies for future applications in human–robot interaction [49, 50].

Different possible compliant joint structures were tested in the UB Hands III and IV. These included different kinds of integrated compliant flexures and similar mechanisms. The last version of the UB Hand III had metal coil springs that went though the fingers and acted as joints, as well as paths for the tendon wires. The ideas were developed further in UB Hand IV, and the final version had joints in the form of torsion springs, made of the same monolithic piece of 3D-printed plastic material as the phalanges [50–52].

SDM Hand

A four-finger (2 vs. 2 fingers) gripper, the SDM Hand, was developed in a Harvard/MIT project. The fingers consisted of elastomeric flexures as compliant joints between rigid polymer links, having embedded sensors and actuation components. They were made using polymer based Shape Deposition Manufacturing (SDM), where the different structural components, made of different materials, were integrated, piece by piece, into complete two-joint fingers [53].

The hand was developed to study manipulation in unstructured environments. It's performance was evaluated in different grasping tasks, involving several different types of objects [53].

RBO Hand

Deimel and Brock [54] developed a simple pneumatic manipulator, called the RBO Hand. Its three fingers were mounted side by side onto a plate, and opposed a palm made from silicone pads. The fingers were made of reinforced, molded silicone rubber, and were pneumatically actuated. They curled when actuated, because one side had been made inextensible [54].

The RBO hand's soft structure and simple actuation made it robust and adaptive, so that it enveloped a grasped object, and held it in a steady grip. The hand was used for research on exploitation of environmental constraints [37, 54].

Molded prosthetic hand for developing countries

A prosthetic hand for developing countries was developed in the University of Genova, in collaboration with the ARTS laboratory of the Sant'Anna University. The hand was made of cheap materials, using simple methods of manufacturing. It had a molded one-piece silicone or polyurethane rubber body, which was based on a cast of a real hand. The compliant flexural joints and tendon wire paths were embedded in the structure during molding [55, 56].

The hand was designed to be either body-powered or EMG-controlled, with only one actuator. The goal was to make it cheap, easy to manufacture, robust, and usable in heavy physical labor. It was only able to perform basic power grasp [55,56].

4.4 Soft systems design and analysis

The previously described soft robotic systems have highly compliant structures and mechanisms as integral parts of their overall morphology. In robotic manipulators, they are usually in the form of compliant joints, or more specifically, monolithic, one-piece flexures, which are used as a replacement for rigid pin-joints. The advantages and disadvantages of using these structures have been listed by e.g. Speich and Goldfarb [57], Howell et al. [58, 59], and Lobontiu [60]. A summary of these listings is presented in Table 3 [57–60].

Main advantages in using compliance as an integral part of a mechanical system, are related to the simplification of the structure in the form of part reduction.

Table 3: Advantages and disadvantages of using compliant joints instead of rigid pin-joints in a mechanical structure [38, 57–60].

Advantages	Disadvantages
• Nonlinear; potential for morphological computation • Component reduction – Less friction, less lubrication – Less backlash – Lower cost – Simplified manufacturing – More space for e.g. sensors • Robust against unpredictable environments • Energy stored in the structure	• Nonlinear; analysis and design difficult • Limited movement range • Center of bending not at the joint center • Poor multi-axial stiffness • Temporal changes in performance – Fatigue – Stress relaxation – Creep • Energy stored in the structure

This leads to several mechanical advantages, e.g. the absence of relative sliding movement between structural components. Thus, no lubrication is needed, which reduces need for maintenance, and makes the device good for applications that require cleanliness. Part reduction also simplifies the manufacturing process and lowers overall cost. Furthermore, through its compliance, the device becomes more robust against unpredictable external forces. There is also more space for sensors due to component reduction, which leads to easier implementation of feedback [57–60].

There are also various disadvantages that need to be taken into account during design. Mainly the geometry and material properties cause limitations and weaknesses. A simple flexure joint, for example, will twist when subjected to torsional loads, and exhibits shear deformation under shear loads. There are also temporal changes in performance due to fatigue, stress relaxation, and creep. All this makes the design and analysis of such nonlinear structure much more difficult, when compared to a rigid, pin-jointed equivalent [57–60].

The recent increase in computing capabilities has given us tools to design and analyze these complex and highly nonlinear systems. The chosen methods depend on the required accuracy, e.g. whether the system is only in the first design stages, or if it needs to be analyzed for durability as an end product. For example topology optimization can be used to find different optimal solutions for producing a

desired output from a defined input load, within a given design space and boundary conditions. Furthermore, finite element analysis (FEA) can be used for analyzing a mechanism's structural integrity, or finding out its response to different loading conditions [58, 59].

Another approach for designing and analyzing these systems is the pseudo-rigid-body model (PRBM). It simplifies the analysis, by regarding the flexible segments as collections of rigid links that are connected by pin joints. Each of the joints has a torsion spring that simulates the force–deflection behavior of the compliant segment. A very simple example can be seen in Fig. 3. To find an equivalent

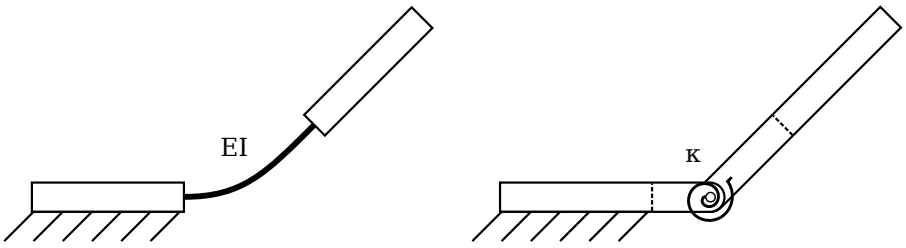

(a) Flexure joint (b) PRBM

Figure 3: A simple pseudo-rigid-body model for a compliant flexure joint between two rigid elements. Force–deflection behavior is modeled with a torsion spring around a pin joint located in a specified point between the rigid elements.

PRBM for a system, one has to decide the amount and placement of the rigid segments and joints, and assign appropriate values for the spring constants. Thus, the complexity and accuracy of the model can be changed intuitively, based on rigid body dynamics [58,61].

Because of its relative simplicity, the PRBM method can be used as an early design tool to analyze systems that undergo large, nonlinear deflections. It can be used for going through several possible designs cost-effectively, without heavy simulations or expensive prototyping. After obtaining initial designs by using the PRBM, one can use numerical methods, such as FEA, or chain algorithm, for more accurate analysis of deflections and stresses in the system [58].

The pseudo-rigid-body model is explained in more detail in Section 6.2 that discusses the modeling of the developed finger prototypes.

Next, we will move on to defining the concept of MorphHand.

5 Concept of MorphHand

The previous chapters gave a compact background for the design of a soft robotic hand prosthesis. Chapter 2 described the human hand's morphology and function to show the complexity of the biological system that a prosthesis should replace. Then, Chapter 3 gave an overview to hand prosthetics and their current development. And finally, Chapter 4 provided a new perspective by discussing morphological computation and its application in soft robotics.

This chapter presents the concept of MorphHand in its current form, and the initial design requirements for its development. First, we will go through the main goals of the concept, and then the performance and physical characteristics of the hand.

But first, let us take a short moment for considering the etymology of MorphHand. It is a combination of the concepts of morphology, morphological computation, morphing, and of course, the human hand. Morphology refers to the structural properties of the device as its main subject matter. Morphological computation is the idea that is being employed in its development. Morphing points to the ambiguous nature of the concept and the device, meaning that the concept will change during its development, and the device can have different forms depending on the individual needs of each user. Finally, the human hand is the main source of inspiration, or the paragon, for developing this device that is supposed to replace it.

5.1 Main objective

The main objective in the development of MorphHand, is to explore the possibility of solving several problems in current myoelectric upper limb prosthetics. This is done by developing a new soft anthropomorphic hand prosthesis, based on the ideas of morphological computation and soft robotics.

The problems, described in Chapter 3, are related to HMI, control, function, and appearance. The main issues in these categories can be described in the following way. Currently, the most used HMI for functional prostheses is the EMG interface, which gives a noisy, difficult to interpret signal through only one or two electrodes. This signal is supposed to be used for controlling a multi-DoF robotic hand, to achieve functionality that is comparable to the human hand. This usually results in a clumsy appearance, and inconveniently slow operation of the device.

The idea that is used for confronting these problems, is morphological computation. The goal is to transfer some of the control, traditionally done by the controller, to the passive dynamic response of the device morphology. The transfer could be done by making the hand from soft, nonlinear materials, to enable the potential for morphological computation, and designing its structure so that it would have similar inherent passive dynamic functions as a real biological hand. Also, its structure should be designed based on mimicking the human hand's trajectories, so that it would have similar inherent passive dynamic functions as its biological paragon. This could result in a more efficient use of the controller's limited computing power, and reduce the effect of the bottleneck formed by the commonly used simple and

noisy EMG interface.

Besides the possibility of simplifying the control requirements, there may be other potential benefits. By mimicking the trajectories and appearance of the human hand, e.g. positioning its joints anatomically correctly in different movements, the hand could be made to behave like the amputee expects, and effectively make its appearance more natural, and its use intuitive and simple. This could make the amputee feel that the device is an integral part of their body. In other words, it would exploit the various phenomena related to how our brain constructs our body image, as described by Ramachandran and Hirstein [62] in their review on the perception of phantom limbs.

In the following, we will take a look at some of the performance and physical characteristics of the proposed device.

5.2 Performance characteristics

The main performance requirement for MorphHand is that it can transfer some of the control to its morphology. Thus, as explained before, its actuated and non-actuated, or passive, motions should mimic the natural trajectories of the human hand. An example is the wrist flexion/extension that causes the passive extension/flexion of the fingers. It should also have a similar compliant response to external forces as a natural human hand. This would make it more robust, and protect it from damage caused by sudden impacts.

The hand should be able to perform at least the main grasp types that were listed in Section 3.1, on page 10. These were lateral, cylindrical, and tripod grasp. Also wrist extension/flexion and rotation should be implemented. It should also have the ability to do basic gestures, like index finger pointing. This leads to the need for individual movement of the thumb, index finger, and middle finger. Thus, the ring and little finger could be connected through their actuation. The fingers' sideways movement could be implemented as spreading them apart in extension, and making them come together in flexion.

Furthermore, the device should adapt to the shape of a grasped object, maximizing the contact area. This would make the grip more stable, and reduces the required force. It would also make grip planning and computation less complex.

5.3 Physical characteristics

One of the main ideas behind MorphHand is that it should replace a lost limb, and make the amputee feel that it is an integral part of their body. Thus, the hand should have a similar shape, size, and appearance as the original, e.g. having the same amount of digits and joints. The basic structure should be easily modifiable and scalable to meet each patient's individual requirements.

But only having the same shape does not lead to the same response. Also the connection between morphology and motor function should be considered. Thus, the structure needs to be designed to enable a similar passive dynamic function as a real hand.

To achieve natural abilities in grasping tasks and other interaction with the environment, as described in Section 2.3, the hand should be soft. The softness should be approximately on the same level as it is in the natural human hand. Also, as mentioned before, the structure should be adaptive, so that it envelops the form of the grasped object as well as possible. These properties could be achieved by using soft, nonlinear materials, and making the structure underactuated.

The main components of the hand could be manufactured as monolithic rubber structures, by e.g. molding or 3D-printing, and the joints could be realized as compliant flexures. This would lead to gaining some of the advantages described in Section 4.4. It would make the hand inherently soft and adaptive. Also, the amount of required parts would be reduced, which would lower costs, and simplify the manufacturing process. Furthermore, the available space to house sensors for feedback could be increased, or the soft material could be made partially conductive, and it could be used as a sensor in itself.

The hand should also be modular, with separate fingers, thumb, palm, and wrist. This way, broken or worn out parts could be easily replaced by changing the module, without having to manufacture a whole new hand. These different modules should be kept simple, easily replaceable, and cost-effective.

Moreover, the compatibility with other existing systems should be considered. First of all, the hand should be compatible with the shoulder prosthesis mechanism developed in the same laboratory [63]. Also, to make the hand's use in prosthetics easier, it should comply with the de facto connector standards in the commercial prostheses (e.g. Otto Bock connectors). This would enable the hand's easier introduction to a user, who already has an existing socket.

In the end, all this should weigh less than the original hand, to make it comfortable to use with the existing socket technologies.

The next chapter will go through the methods that were used in this thesis to explore the possibility of realizing the described concept

6 MorphHand finger prototypes

This chapter describes the process of designing and testing finger prototypes for MorphHand. The topic was originally discussed in a conference paper for IEEE ROBIO 2012 [64]. In this thesis, the reader is given a more complete, broader perspective to the design process and further developments.

The prototypes were manufactured to test a possible structure for MorphHand's fingers, and to explore the possibility of producing them, and possibly the whole hand, with the methods that were available. The available tools were: an Artec 3D M scanner, Dassault Systèmes SolidWorks CAD/simulation software, a CAM/CNC milling machine, and a 3D-printing service provided by a collaborating company, called Three Esu (SSS) Co. Ltd.

First, Section 6.1 describes the prototype design process from initial tests to defining the structure and morphological parameters for different prototype versions. Next, Section 6.2 takes us through the modeling considerations for predicting the prototypes' response based on the different parameters. And finally, Section 6.3 gives details on the measurement methods that were used for finding out their actual response.

6.1 Finger design

The design process included initial tests for finding out the possibilities of the chosen manufacturing methods and materials. After the tests, a simple base structure was designed. It was then modified to create several prototypes for testing different morphological parameters and their effect on the response. Finally, these prototypes were 3D-printed to be evaluated in bending tests that are described in Section 6.3.

6.1.1 Initial tests

An initial prototype was created to test the chosen manufacturing methods, starting from scanning a real finger, to printing a real scale rubber copy with functional modifications.

A human male's right hand was 3D-scanned with the Artec 3D M scanner. This was done in a similar fashion as Saito et al. did in 2005 [15], but scanning the hand directly, and thus excluding the intermediate phase of making a plaster model. The hand was fixed in place with plastic tubing and tape, and the subject kept his index finger straight and slightly separated from the other fingers while it was scanned. Geometry of the index finger (Fig. 4) was extracted from the data and transferred to be modified in CAD (SolidWorks).

Measuring from the acquired 3D data, the scanned finger was approximately 20 mm wide at the PIP joint, and 18 mm from the DIP joint. The phalanx bone lengths were approximated to be 45 mm for proximal, 25 mm for medial, and 22 mm for distal phalanx. Overall finger length (MCP joint to fingertip) added up to 95 mm, including the soft tissues in the tip. These measures are prone to error, because the locations of the joints were approximated based on the outer contours of the finger.

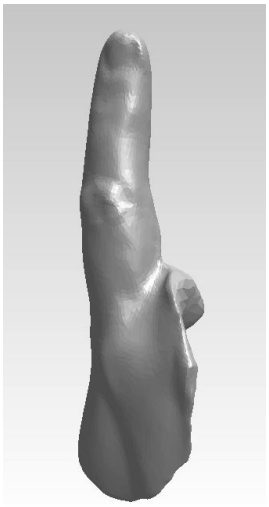

Figure 4: 3D-scan of an adult male's index finger. The finger is slightly bent to the right.

But, comparing to the results in a study by Buryanov et al. [65], it was confirmed that the measured proportions of the sample finger were within normal range.

The MCP joint, and approximately a third of the proximal phalanx, were excluded at this point by cutting the model at the MCP crease that separates the palm from the finger. This simplified the structure and reduced the material requirements for printing prototypes. Also, a supporting base and some inner structures, for tendon wires and connection pins, were added in CAD.

The CAD model of the first prototype finger was sent to Three Esu (SSS) Co. Ltd., which 3D-printed it from a rubber-like polymer using their LB-313J printer. The resulting model is shown in Fig. 5. The material was called VLX-848 'rubber-like', and it was provided by the company. Its known properties are given in Table 4. Different additives could be blended in to change color, physical properties, or conductivity. Furthermore, it is important to note that material hardness depended on intensity of the curing light in the printing process.

Table 4: Given material properties for VLX-848 'rubber-like' polymer [66].

Property	Value
Tensile strength (MPa)	1.68
Elongation at break (%)	120
Glass transition (°C)	55
Color	light, transparent
Shore hardness (durometer, type A)	60

Figure 5: The first 3D-printed prototype finger.

The printed prototype was compared to the original finger, and the general shape and dimensions were confirmed to be the same. Only a small overall shrinkage due to the printing process was observed. The results proved that it was possible to use the process to print the wanted functional structures. Also, the material seemed suitable to be used in the planned device, based on a qualitative examination.

This worked as a basis for designing the next prototypes.

6.1.2 Prototype structure

A simple rectangular notch joint structure, as in Fig. 6, was chosen to be implemented for the PIP and DIP joints. The geometry was kept simple to make quantitative analysis easier. As a result, basic beam equations could be used to approximate the changes in stiffness and strength, when changing joint dimensions. This is discussed in more detail in Section 6.2.1. The maximum structural angles for the joints were chosen to be 90° for PIP and 80° for DIP. This followed the natural relative maximum angles of a real finger, while being smaller for practical reasons. Also the inner structures were developed further to make the assembly of the components easier, i.e. inserting the horizontal pins and tendon wires. Basic structural simulation (SolidWorks Simulation) was used to confirm the function and stress concentrations of the joint structure.

The MCP joint was not included, due to its 2 DoF structure, to simplify the analysis and reduce the material requirements for 3D-printing. Including it as a 1 DoF joint would have made it equal to the two others. This would have been redundant with regard to analysis of the chosen parameters. Thus, the implementation of a 1 or 2 DoF MCP joint was left as future work.

Overall eight different configurations were derived from the basic structure to see the effect of the chosen morphological parameters. These parameters were the width

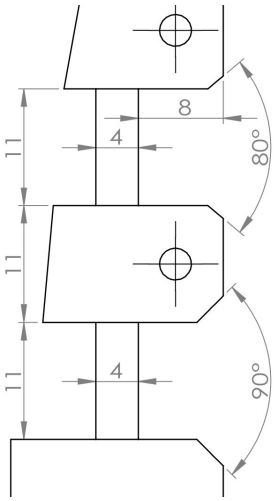

Figure 6: Basic joint structure for the prototypes.

and thickness of the compliant joint, the material hardness, and the experimental air pocket structures around the joints. The different configurations are listed in Table 5.

Table 5: Prototype finger configurations.

Configuration	t_{pip} mm	t_{dip} mm	w^*_{pip} mm	w^*_{dip} mm	Material	Air pockets**
02a	4	4	20	20	hard	–
02b	5	4	20	20	hard	–
02c	4	4	20	17	hard	–
03a	4	4	19 . . . 20	17 . . . 18	soft	fbPIP, fbDIP
03b	4	4	19 . . . 20	17 . . . 18	soft	bPIP, bDIP
03c	4	4	19 . . . 20	17 . . . 18	soft	bPIP
03d	4	4	19 . . . 20	17 . . . 18	soft	–
03e	4	4	19 . . . 20	17 . . . 18	hard	–

t = thickness, w = width.
*03a–c had a 1 mm width difference between joint top and bottom.
**Pocket locations: f = front of the joint, b = back of the joint.

The morphological parameters were chosen based on their assumed effect on the fingers' response, i.e. their trajectory in a free flexion-extension cycle. Thus, the parameters that were connected to the joints' stiffness, and the stiffness ratio between them, were deemed important. The ratio of dimensions between the joints affects their stiffness ratio, which in turn determines their bending order, and thus the overall trajectory of the finger. The maximum structural joint angles, on the

other hand, limit the trajectory. Finally, the compliant function of the finger comes fundamentally from its material properties, which makes them perhaps the most important parameter. However, only a comparison between a hard and soft version of the same material could be done, due to lack of data on the used material's properties.

The different configurations were implemented by printing five prototype fingers. One of them (03a-d), shown in Fig. 7, was printed from a softer version of the material. It had a more natural, or anthropomorphic, shape with ≥ 1 mm thick

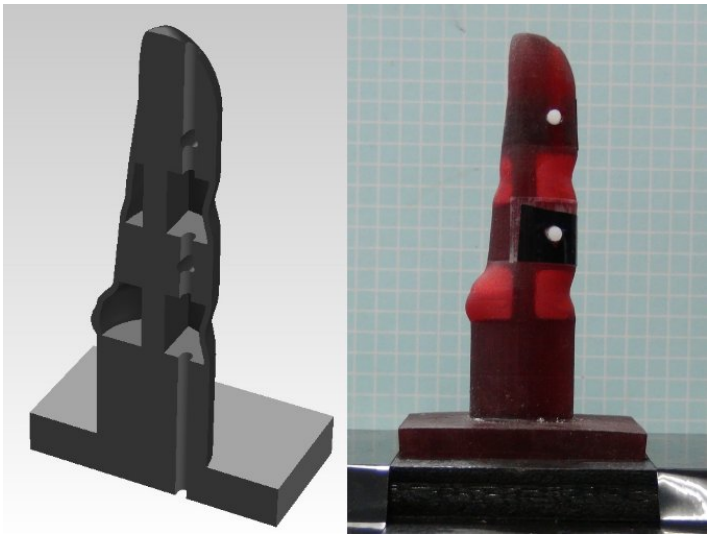

Figure 7: Prototype with closed air pockets around the joints.

'skin' structures on both sides of each joint. These were made of the same monolithic piece of material as the rest of the finger. On the back of each joint they formed an enclosed space containing air, and in the front, they covered the tendon wire sliding in the joint opening. This single prototype counted as four different configurations, because its air pockets were cut open one by one in the test procedures to see their effect. The four other fingers were made of harder rubber material, one serving as a reference (02a), one having a thicker PIP joint (02b), and another a narrower DIP joint (02c), and the last (03e) having the same shape as the soft one, but without the air pockets.

All the prototypes had two horizontal holes, one in the distal part, and one in the medial. Their purpose was to accommodate the pins (Fig. 8) for attaching the tendon wires. The pins were designed in CAD and manufactured from plastic by using a computer numerical controlled (CNC) milling machine.

The next section will take a look at the modeling considerations for analyzing the described prototypes.

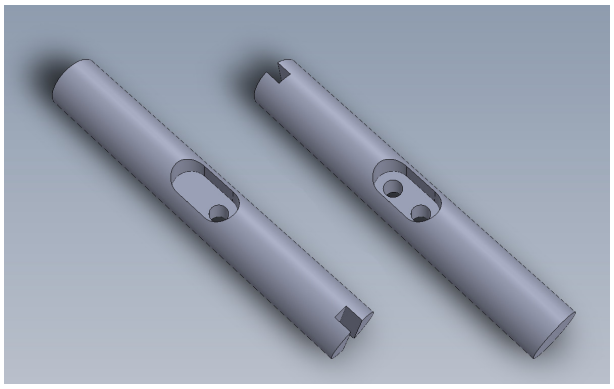

Figure 8: CAD model of the horizontal pins for attaching the tendon wires.

6.2 Modeling

This section describes the different methods that were used for analyzing the developed basic prototype structure. First, the effect of changes in relative stiffness between the joints is approximated by using basic beam equations. Then, a basic pseudo-rigid-body model is derived for the prototype structure, to be used as a design tool for further development.

6.2.1 Approximation of relative joint stiffness

The Euler–Bernoulli (EB) beam theory was used to initially approximate the differences in the prototypes' response. The EB equation states that the bending moment of a beam is proportional to its curvature:

$$M = k\frac{d\theta}{ds}, \tag{1}$$

where M is the moment, k is the stiffness of the beam, and $\frac{d\theta}{ds}$ is the rate of change in angular deflection, i.e. the curvature. The stiffness k of a beam is a function of material properties and geometry:

$$k = EI, \tag{2}$$

where E is Young's modulus, which depends on the material properties, and I is the second moment of area, which describes the cross-sectional geometry of the beam with regard to an arbitrary axis [58].

The prototype fingers had a simple rectangular notch joint, and for a beam with a rectangular cross-section, we have:

$$I = \frac{wt^3}{12}, \tag{3}$$

where w is the width and t is the thickness of the joint [58].

The material is assumed to be homogeneous, i.e. Young's modulus is same for both joints. Thus, their relative stiffness depends only on the geometry. From this we get the relation K between DIP and PIP joints:

$$\frac{k_{dip}}{k_{pip}} = \frac{I_{dip}}{I_{pip}} = \frac{w_{dip}t_{dip}^3}{w_{pip}t_{pip}^3} = K, \tag{4}$$

which shows the effect of changing the basic geometry of the joints. If we assume that stiffness is the major contributor to the joints' order of bending, and other factors, such as friction in the actuating wire, are negligible, we can come to the conclusion that

$$K = \frac{1}{m}, \tag{5}$$

where m is the slope of a graph showing PIP joint angle as a function of DIP joint angle.

Now, we can calculate K, and the equivalent m, for the two prototypes that were designed to have a difference in stiffness between the joints (02b and 02c in Table 5, on page 29). For prototype 02b:

$$K_{02b} = \frac{20 \cdot 4^3}{20 \cdot 5^3} \approx 0.51,$$

$$m_{02b} = \frac{1}{K_{02b}} \approx 1.95,$$

and for 02c:

$$K_{02c} = \frac{17 \cdot 4^3}{20 \cdot 4^3} = 0.85,$$

$$m_{02c} = \frac{1}{K_{02c}} \approx 1.18.$$

Thus, for prototype 02b, the bending speed for PIP joint should be approximately 50 % slower than for DIP joint. For prototype 02c this difference should be 15 %.

Due to the assumptions used in the Euler-Bernoulli beam theory, it only applies to small deflections. Thus, it can only be used to approximate the relative stiffness of the joints. A different way of modeling the finger kinematics is required. In the next section, we will derive a pseudo-rigid-body model for the prototypes for this purpose.

6.2.2 Pseudo-rigid-body model

Here, an initial pseudo-rigid-body model (PRBM) is derived for the prototype fingers to approximate their kinematics. Its purpose is to find the two-dimensional relationship between the wire displacement, joint angles, and fingertip location. The model can then be used for design purposes in the future.

We will start by approximating the bending of a single cantilever beam by using a PRBM with one rotational DoF (1R). This is used for a single compliant joint. After that, we can expand the model to include the whole prototype with both joints, the rigid links between them, and the tendon wire.

Several assumptions will be made while deriving the model. We will assume that the phalanges are completely stiff, and that the joints deform always in the elastic range, without shear. The joints are also required to have homogeneous material properties, and a constant, rectangular cross section, for the cantilever beam analogy to function properly [58].

So, let us consider a simple cantilever beam that has a moment at the free end, as in Fig. 9(a). Its tip follows a nearly circular path, with some radius of curvature along the beam's length. We can use this information for approximating the tips path with a PRBM [58].

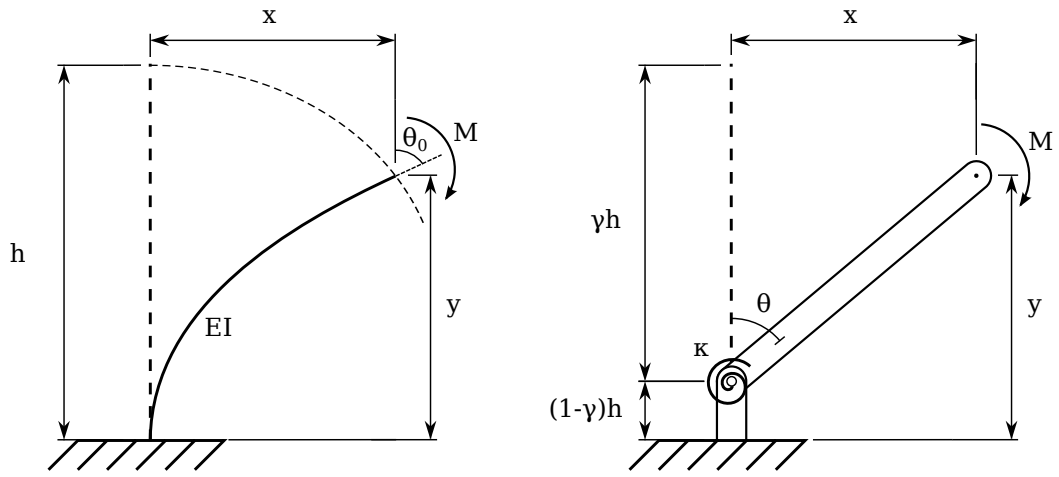

(a) Cantilever beam with moment at free end.

(b) 1R PRBM.

Figure 9: Simplified model for a cantilever beam, using the pseudo-rigid-body model.

The motion of the beam under load is approximated by replacing the flexible beam with two rigid links that are connected through a pin-joint with a torsion spring, as in Fig. 9(b). Here, γ is the *characteristic radius factor* that defines the location of the pin-joint in the PRBM, and θ is the *pseudo-rigid-body angle*. From these we can get the tip coordinates:

$$x = \gamma h \sin\theta \tag{6}$$

$$y = (1-\gamma)h + \gamma h \cos\theta \tag{7}$$

The relation between the actual beam angle and the pseudo-rigid-body angle, is defined by the *parametric angle coefficient*, c_θ, as:

$$\theta_0 = c_\theta \theta \tag{8}$$

The *torsion spring constant*, κ, is defined as:

$$\kappa = \gamma \kappa_\theta \frac{EI}{h}, \tag{9}$$

where κ_θ is a stiffness coefficient. And finally, the *maximum stress*, σ_{max}, which occurs at the fixed end, is given as:

$$\sigma_{max} = \frac{Mt}{2h}, \tag{10}$$

where t is the thickness of the compliant rectangular beam [58].

Howell [58] gives an approximation for the parameters of a PRBM with a moment in the free end, by defining:

$$\gamma = 0.7346,$$

$$c_\theta = 1.5164,$$

$$\gamma\kappa_\theta = 1.5164$$

By substituting these to the previous equations, we get:

$$x = 0.7346h\sin\theta \tag{11}$$

$$y = h[1 - 0.7346(1 - \cos\theta)] \tag{12}$$

$$\theta_0 = 1.5164\theta \tag{13}$$

$$\kappa = 1.5164\frac{EI}{h} \tag{14}$$

Now we have a simple 1R PRBM for a single joint. By combining two of them in series, with appropriate structural dimensions, and adding a tendon wire, we get a model for a full two-joint prototype finger, as shown in Fig. 10.

For the fingertip of this 2-DoF system, we get the basic forward kinematic equations as:

$$\begin{bmatrix} x_t \\ y_t \\ \phi_t \end{bmatrix} = \begin{bmatrix} l_2\sin\theta_1 + l_3\sin(\theta_1+\theta_2) \\ l_1 + l_2\cos\theta_1 + l_3\cos(\theta_1+\theta_2) \\ \theta_1+\theta_2 \end{bmatrix}, \tag{15}$$

and the differential relationship between the joint displacements, and resulting fingertip motion, by calculating the Jacobian matrix for the system:

$$\mathbf{J} = \begin{bmatrix} \frac{\partial x_t}{\partial\theta_1} & \frac{\partial x_t}{\partial\theta_2} \\ \frac{\partial y_t}{\partial\theta_1} & \frac{\partial y_t}{\partial\theta_2} \\ \frac{\partial\phi_t}{\partial\theta_1} & \frac{\partial\phi_t}{\partial\theta_2} \end{bmatrix} \tag{16}$$

$$\begin{bmatrix} \dot{x}_t \\ \dot{y}_t \\ \dot{\phi}_t \end{bmatrix} = \mathbf{J}\begin{bmatrix} \dot{\theta}_p \\ \dot{\theta}_d \end{bmatrix} = \begin{bmatrix} l_2\cos\theta_p + l_3\cos(\theta_p+\theta_d) & l_3\cos(\theta_p+\theta_d) \\ -l_2\sin\theta_p - l_3\sin(\theta_p+\theta_d) & -l_3\sin(\theta_p+\theta_d) \\ 1 & 1 \end{bmatrix}\begin{bmatrix} \dot{\theta}_p \\ \dot{\theta}_d \end{bmatrix} \tag{17}$$

Also, by looking at Equations 4 and 14, we can see that the joint stiffness ratio, K, which was derived in Section 6.2.1, is equal to the ratio of the rotation spring constants. By combining these equations, we get:

$$K = \frac{k_{dip}}{k_{pip}} = \frac{\kappa_2}{\kappa_1} = \frac{w_2t_2^3}{w_1t_1^3} \tag{18}$$

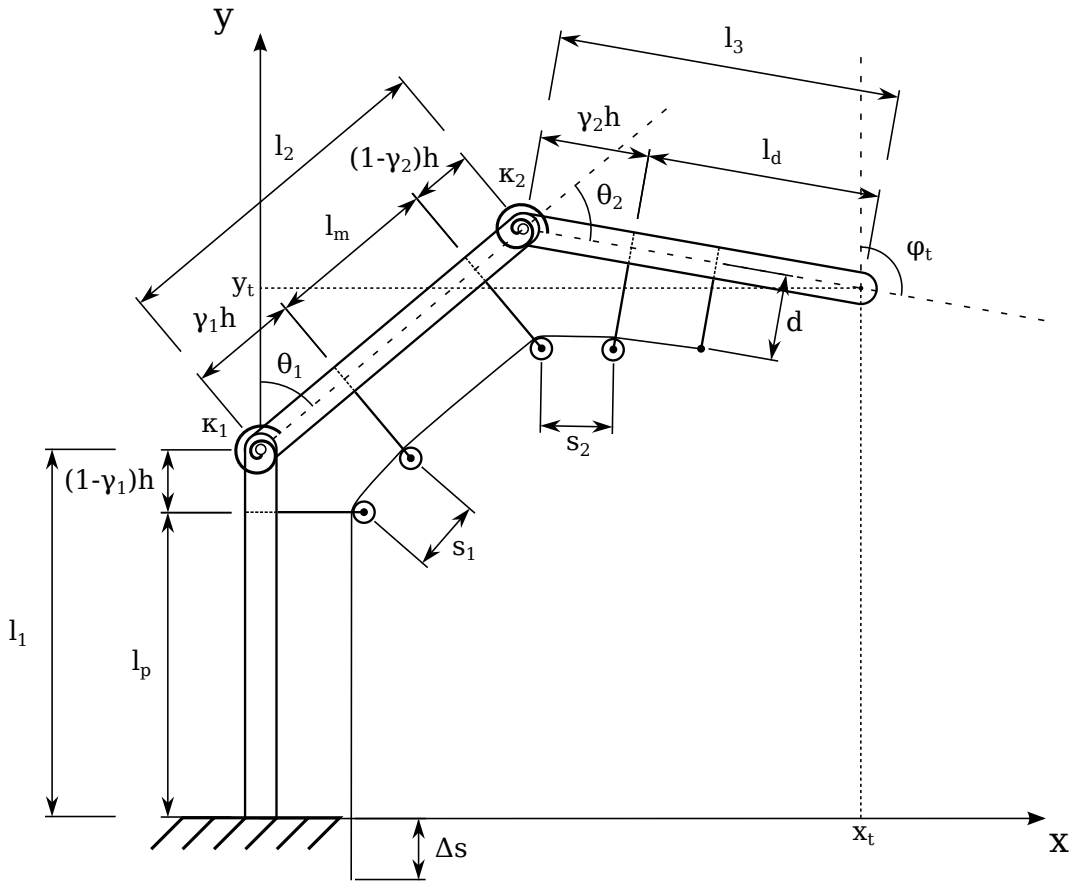

Figure 10: Three-link two-joint PRBM for the prototype fingers, with tendon wire displacement.

Now we have gone through the initial steps in describing the prototypes' kinematics, and given a solid basis for modeling the prototype fingers in a computer simulation. Still, the relation between the tendon wire displacement, joint angles, and fingertip location need to be solved to make the model work as intended. Furthermore, while the proposed 1R joint model can be used to approximate the trajectory of a single compliant beam, it may be too inaccurate for the designed two-joint finger structure. Besides getting the fingertip to follow the same trajectory as the actual prototype, it is important to have the phalanges in the same angle. The angular accuracy can be increased by increasing the amount of rigid links in the PRBM, i.e. making it 2R, 3R, and so on. As shown by Feng et al. [67] and Su [61], the 2R and 3R PRBMs can be used to increase accuracy noticeably.

However, we will stop here, and leave further derivations of the model, and its validation against the measurement results, as future work. We will move on to the next section, which will describe the prototype measurements.

6.3 Measurements

Here, we will go through the series of measurements that were done to test the feasibility of the developed prototype mechanism, and the ideas behind the MorphHand concept.

The five prototype fingers were tested in bending tests in the eight configurations described in Section 6.1.2. The goal was to see how the joint thickness and width, the material hardness, and the air pockets affected the prototypes' response. The measurements were done in two parts using a motion capture system. The first part evaluated the prototypes' overall function and response relative to a measurement on a real human index finger. The second was done to get more accurate data on the prototypes' trajectories. Also, a simple force measurement was done to see the required forces for bending the fingers.

6.3.1 Motion capture

The finger bending measurements were done using a 3D motion capture system with two cameras (Library Co. Ltd.). The cameras were located in a pole with one approximately 0.5 m above the other. The distance to the measured finger was also approximately 0.5 m.

A 10 cm x 10 cm x 10 cm reference marker cube, shown in Fig. 11, was built for the motion capture measurements. It had overall 26 reflective markers on four sides, nine on two sides, and four on the other two. The cube was used to calibrate the camera system before each measurement session. The average error for the marker locations in the calibration was 0.57 mm with a standard deviation of 0.41 mm.

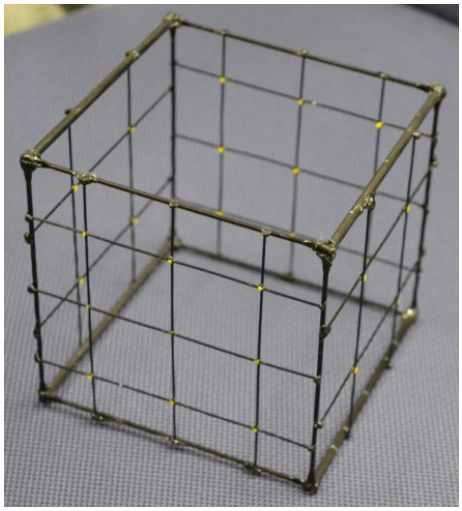

Figure 11: Reference cube with reflective markers for the motion capture measurements.

For the measurements, markers were placed on one side of the measured fingers. In the first measurements, the fingers' base, joint centers and tip were marked

with reflective tape (Fig. 12). Four markers were added for the second measurements, above and below the joints (Fig. 13). This led to a more accurate and direct measurement of the joint angles.

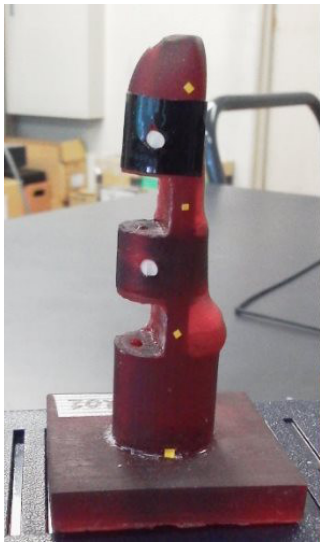

(a) Prototype with air pockets cut from the front (02b).

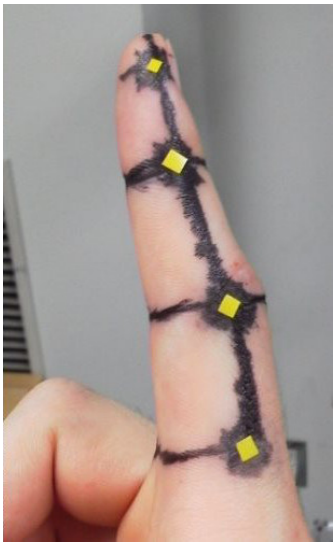

(b) Human index finger.

Figure 12: Placement of the four markers in the first motion capture measurements. Black marker pen was used to enhance contrast with the subject's skin.

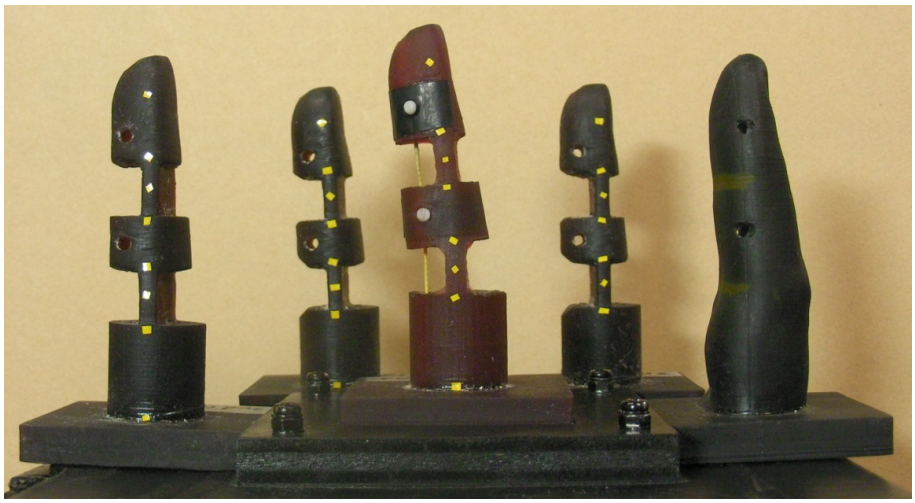

Figure 13: Marker placement in the second measurements. The remaining prototypes from left to right: 03e, 02a, 03d, 02c, and 01.

The fingers were actuated by one DC servo motor that pulled one tendon wire connected to the horizontal pin in the distal phalanx (Fig. 14). A steel wire with

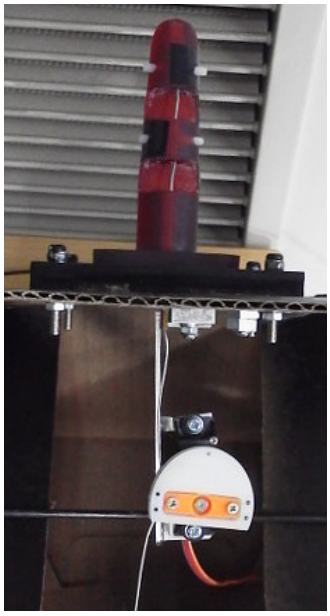

Figure 14: The actuation setting for bending the rubber fingers.

a polymer coating was used in the first measurements, but later it was changed to a lighter and more flexible coated string. This reduced the possible trajectory restricting effects of the wire's rigidity and weight. The pin in the medial phalanx was also inserted, but it only worked as a support for the wire.

The servo motor was controlled with a pulse-width modulation (PWM) signal from a Texas Instruments MSP430 microcontroller. A simple breadboard circuit enabled the finger to be bent either manually by using a potentiometer, or automatically by pressing a button. When the button was pressed, the prototype was pulled once from a fully straight position to approximately full flexion in 6 s. After this, the finger was released in the same time interval to pull itself up with the energy that had been stored in the compliant structure.

In the first part of the measurements, one flexion-extension cycle was recorded at 30 frames per second for all of the configurations. The effect of the air pocket structure was tested by cutting the rubber skin off, part by part, between measurements. The finger was first measured with all air pockets. Then, both front pockets were cut off simultaneously, then the DIP backside pocket, and finally, the PIP backside pocket.

The reference measurement on a human male's right index finger was done with the forearm, wrist, and MCP joint supported by a wooden board up to the PIP joint. The four markers were placed in the same fashion as for the rubber fingers (Fig. 12), to the base of the finger, approximately on the center of rotation in the joints, and the tip. 11 consecutive flexion–extension cycles were recorded with the motion capture system.

Only four fingers with four configurations (02a, 02c, 03d, and 03e) remained for the second part of the measurements, which was done several months later. The

soft finger with air pockets (03a–c) had been cut, and the one with a thicker PIP joint (02b) had become unusable due to material failure. A quickly growing fracture had appeared in the back of its joint in the area of highest stress concentration. A minimum of 10 flexion–extension cycles were recorded for each of the remaining four fingers.

6.3.2 Bending force

Simple force measurements were done to see the approximate force required for bending the fingers to maximal flexion in under a second. Less than 1 s flexion time was determined to be reasonable, based on the review Belter et al. had made on the performance specifications of anthropomorphic prosthetic hands [34].

The prototypes were placed on a rigid metal stand with a hole under it. A recording force gauge (Imada ZPS-DPU) was attached to the tendon wire, which in turn was connected to the distal phalanx of the finger. The second horizontal pin was also inserted for support, as in the previous measurements.

The fingers were pulled manually to maximum flexion in less than 1 s, repeating a minimum of five times. The maximum forces were recorded and the average maximum force required for maximal bending was determined. Clearly outlying measurement results were discarded and the gauging was repeated.

6.3.3 Data analysis

The marker locations in Cartesian coordinates were acquired from the motion capture images using the program provided with the system (Move-tr/3D, Library Co. Ltd.). Smoothing was used to eliminate higher frequency disturbances, caused by e.g. friction in the wire and DC servo motor backlash.

The extracted data was analyzed using MATLAB. For the second measurements, an average of the marker location data was calculated for the recorded ten or above flexion–extension cycles. The first measurements had only one recorded cycle, and no averaging was used. The trajectories were calculated by using simple translations and rotations. The base marker on the proximal phalanx was used as a reference and it was translated to origin for each point of time. All the other marker locations were then translated relative to that point, and rotated relative to the axes. Finally, the slight sideways variation was eliminated by projecting the trajectory to xy-plane.

The joint angles were calculated as the angles between vectors formed by the markers. Because there were only four markers in the first measurements, the results were affected by joint center movement, and the PIP and DIP joint angles had a dependency. This was corrected in the second measurements, by using the four additional markers above and below the joints.

7 Prototype test results

The results of the first measurements were presented originally in the IEEE ROBIO 2012 conference [64]. Those results were revised for this thesis, and several corrections were made based on additional data gathered from the second measurements.

This chapter is organized according to the analyzed morphological parameters. First, Section 7.1 presents the results related to the changes in joint geometry. Then, Section 7.2 continues by giving an overview on the material's effects on the prototypes' response. And finally, Section 7.3 describes the effects of the experimental air pocket structure.

7.1 Joint geometry

The acquired measurement data shows the effect of changing the joint geometry on the prototypes' response. Fig. 15 shows the trajectory and joint angle graphs for the reference prototype (02a), and the ones with modified joint thickness (02b) and width (02c). For comparison, Fig. 16 shows the results for the measured human index finger. Approximate slopes for free flexion and extension were obtained from these graphs, as presented in Table 6. The force measurement results for all the prototypes are presented in Table 7.

Table 6: The predicted and obtained slopes for the real finger and the prototypes with differences in joint thickness and width (02a–c).

Finger	Predicted slope	Flexion slope	Extension slope	Note
Real	$1.00 \pm 0.31^{*}$	1.15	1.15	
02a	1.00	0.65	1.12	Reference
02b	1.95	1.07^{**}	1.70^{**}	+25 % PIP thickness
02c	1.18	0.75	1.38	−15 % DIP width

*From Leijnse et al., 2010 [9].
**Use of only four markers caused PIP and DIP joint angles to have a dependency.

Comparing the graphs and slopes for configurations 02a–c, in Fig. 15 and Table 6, it is clearly visible that both PIP thickness increase by 1 mm and DIP width decrease by 3 mm affected the joint stiffness, and caused the DIP joint to bend faster than the PIP joint. The rubber fingers' graphs also show a clear hysteresis between flexion and extension, which is not the case with the real finger.

Furthermore, from Table 7 we can see that the prototype with the thickest joint (02b) required the most force for bending it. The 25 % thickness increase made the PIP joint much stiffer, resulting in a maximum force of ≤ 15 N.

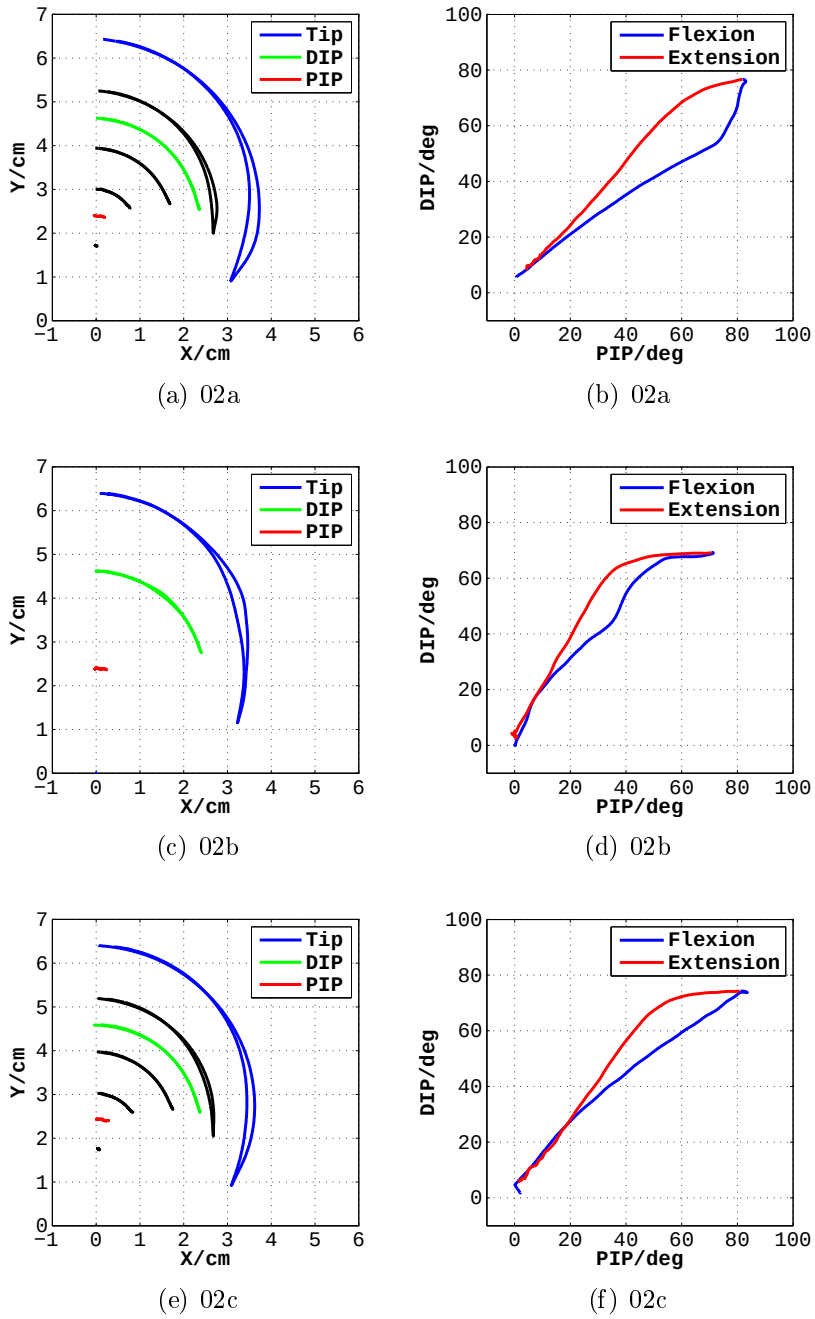

(a) 02a (b) 02a

(c) 02b (d) 02b

(e) 02c (f) 02c

Figure 15: Result graphs for prototypes with different joint thickness and width (02a–c). Prototype 02b was measured only with four markers.

As for the real finger, there is a clear overextension past the neutral straight position. This can be seen as a negative finger tip location, and a negative DIP joint angle in the beginning. Also a slight curve is observed in the end of flexion, which is most probably caused by the tightening of PIP flexion, when the DIP joint is already at its maximum. At this phase, the fingertip and the medial phalanx press

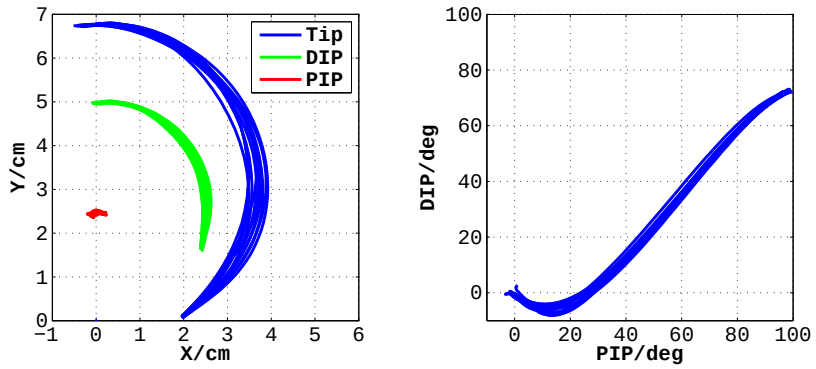

(a) Real (b) Real

Figure 16: Result graphs for the real finger.

Table 7: Force measurement results for each prototype. Average maximum bending force from full extension to full flexion, in $t \leq 1$ s.

Finger	Average max force (N)	Note
02a	≤ 13	Reference
02b	≤ 15	+25 % PIP thickness
02c	≤ 11	−15 % DIP width
03a	≤ 10	All pockets
03b	≤ 10	Front cut
03c	≤ 7	DIP cut
03d	≤ 6	All open, soft
03e	≤ 12	All open, hard

against the soft tissues of the proximal phalanx. Between these two anomalies, the joint angle curve has a constant slope. These results coincide with the ones Hahn et al. got in their in vivo study on the linkage between the index finger's IP joints [10].

The displacement of the MCP joint marker, seen in the trajectory graph in Fig. 16(a), is partly caused by soft tissues compressing under it. Also, the joint did have some freedom of movement, because the proximal phalanx was hard to fix in its place completely.

7.2 Material

The effects of material hardness on the prototypes and their response were easily observable. This can be seen from the force measurement results, in Table 7, and the graphs for the two prototype configurations, 03e and 03d, with the same structure, but different material stiffness, in Fig. 17.

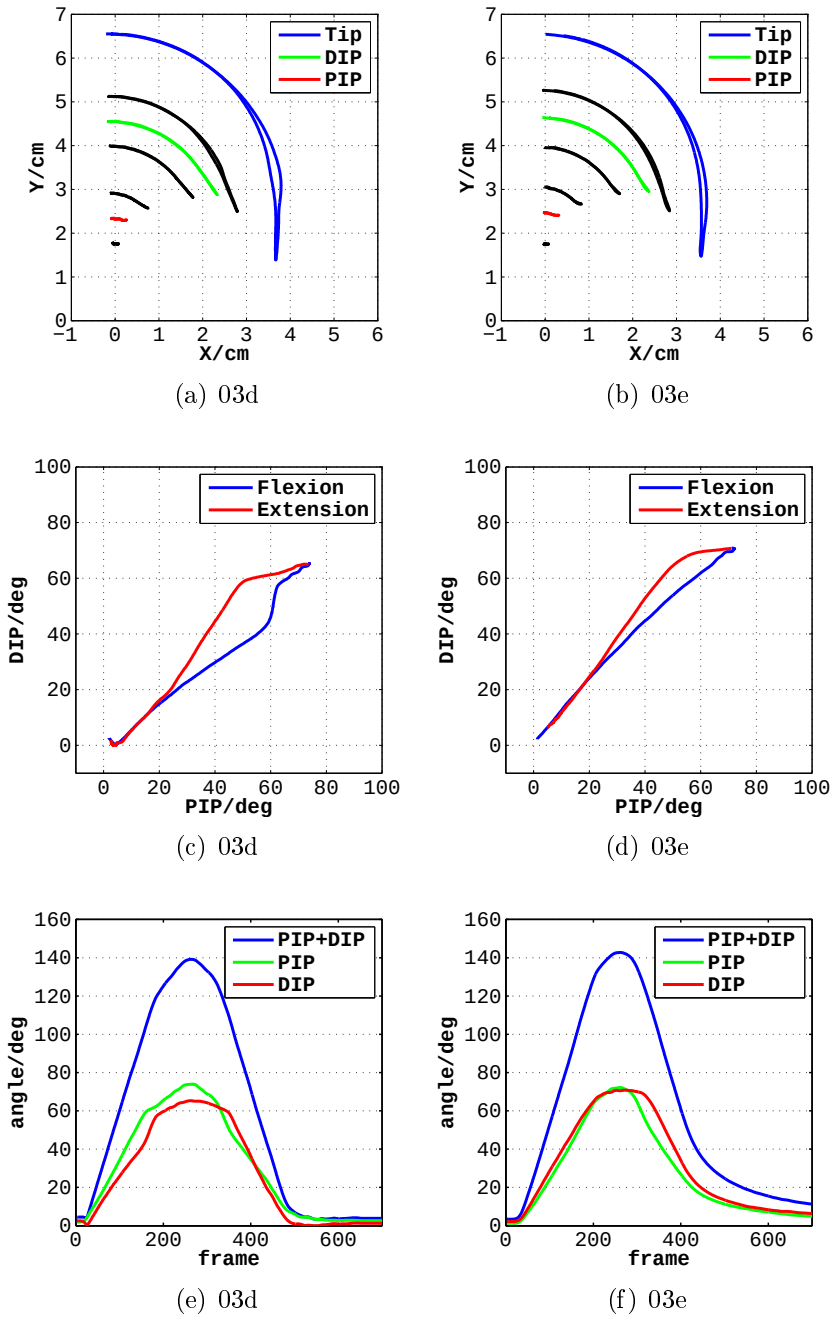

(a) 03d (b) 03e

(c) 03d (d) 03e

(e) 03d (f) 03e

Figure 17: Result graphs for the geometrically equal prototypes made of soft (03d) and hard (03e) material.

First of all, there was a major difference in the forces between the prototypes made of either soft or hard version of the same material. As seen in Table 7, all the hard fingers (02a–c and 03e) had a required bending force of over 10 N, while the soft one (03a–d) reached this limit only by having the air pockets. Of the two equal fingers, the softer one, 03d, had the average maximum force of ≤ 6 N, while

for 03e it was doubled, i.e. $\leq$ 12 N. During the force measurements, a clear stress relaxation was also observed in all the fingers, i.e. the force that was needed to keep the fingers in full flexion reduced with time.

When comparing the trajectory graphs for the two geometrically equal prototypes (Fig. 17(a) and 17(a)), it seems that there is little or no difference. However, the joint angle graphs (Fig. 17(c)–17(f)) show that their behavior, especially close to full flexion, is quite different. First, the soft finger shows a wider hysteresis, and exhibits a wavy movement pattern in full flexion. This is most probably caused by the compression of the soft finger's structure on itself, as recorded in Fig. 18. The harder finger did not yield as easily, and its response was much more linear. On the other hand, from the graphs we can see that the soft finger returned to full flexion directly, while the harder prototype's response started to become slower towards the end. This happened approximately 40 degrees before full flexion.

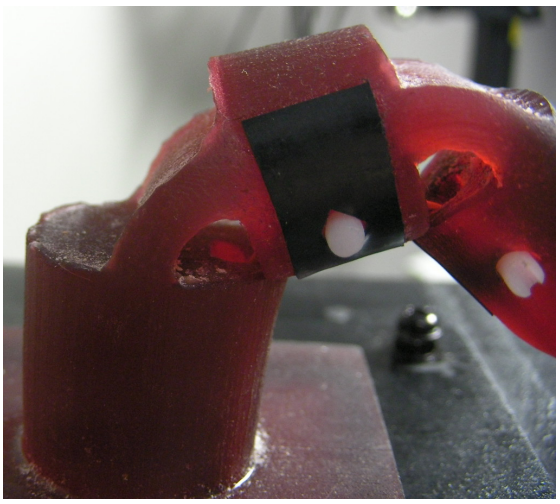

Figure 18: The soft prototype (03d) compressing on itself in full flexion.

In the end, most of the fingers made of harder rubber showed material failures after repetitive bending motions. The most affected areas were the ones with highest stress concentrations, i.e. the upper and lower parts in the back of the joints. Especially configuration 02b, with a thicker PIP joint, had a rapid material failure in the upper edge of the joint during the cyclic force measurements. Fig. 19 shows the reference prototype, 02a, which showed a similar failure several months after the second measurements.

These failures were observed in the softer prototype (03d) only after two years had passed from its printing. During this time, it had been subjected to different environmental and lighting conditions, and gone through at least over a hundred full bending cycles in many different directions. Other observed material failures in the soft finger were caused by the tendon wire cutting through the front skin structure, and the initially too large horizontal pins slightly ripping the sides of their insertion holes.

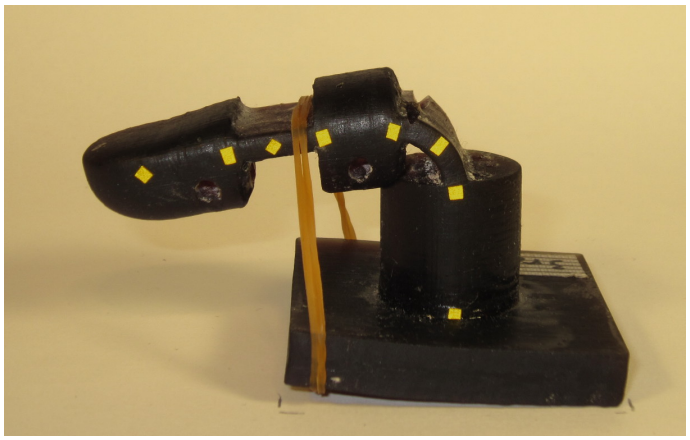

Figure 19: Reference prototype (02a) showing serious structural failure months after the second measurements.

7.3 Air pockets

The air pocket structure was designed to give the finger a more anthropomorphic shape and to see how it affected the response of the finger, especially due to the closed air pockets it formed behind the joints.

The effect of the skin structure on the prototype's response can be seen when comparing the trajectory and joint angle graphs for configurations 03a–c, with the air pockets, in Fig. 20, and 03d, which had all of them cut off, in Fig. 17. The trajectories show a clear movement restricting effect, especially when comparing 03a to 03b with and without the skin structure in the front, respectively, and 03c to 03d with just a PIP air pocket and without air pockets, respectively.

Especially the PIP backside pocket had a major effect on the joint angles. The DIP joint bends first to near maximum, and PIP follows after this. Also the hysteresis, which was apparent in the other configurations, became very small, because the air pocket pulled the finger up in unison with the release of the tendon wire.

This concludes listing of the main results that were acquired from the different measurements. In the next chapter, we will discuss their implications.

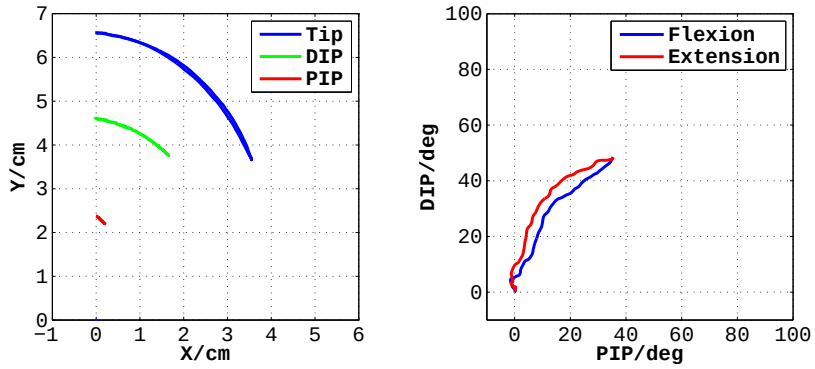

(a) 03a

(b) 03a

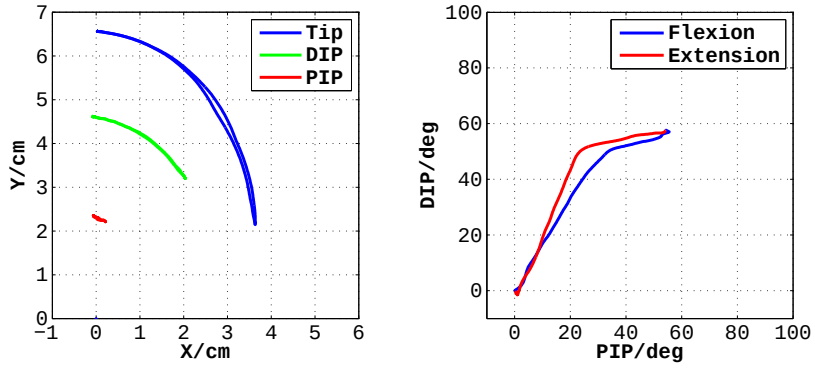

(c) 03b

(d) 03b

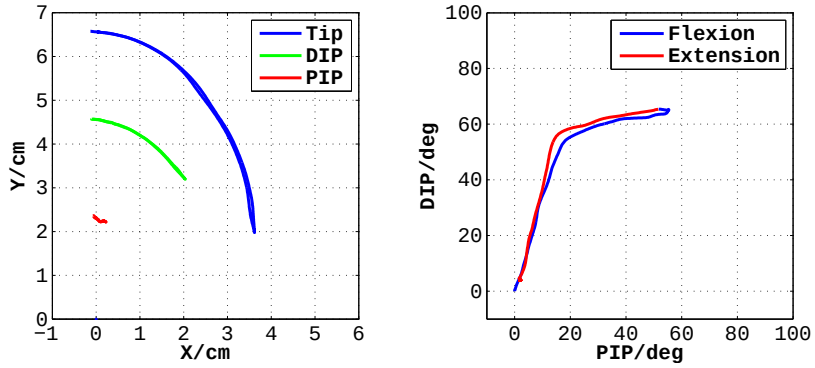

(e) 03c

(f) 03c

Figure 20: Result graphs for the configurations with air pockets around the joints. 03a had all pockets, 03b was open from the front, and 03c had only the PIP backside pocket left.

8 Discussion

In this chapter, we will discuss the main observations that were made based on the presented measurement results. We will first go through the effect of the tested morphological parameters, then consider the results in the context of the proposed concept, and finally go through some of the future steps that could be taken in the development of MorphHand.

8.1 Morphological parameters

The results show that the considered morphological parameters, joint width and thickness, material hardness, and the air pocket structures, could be used to adjust the fingers' response to the desired direction. Here we will discuss how.

Joint geometry

As described previously, in Section 6.2.1, the relative stiffness between the two compliant joints should have had a clear effect on their order of bending. The assumption was, that the relation would indicate the inverse of the slopes in graphs presenting the PIP joint angle as a function of DIP joint angle.

Based on the results, changing the stiffness ratio, K, did cause a response change to the expected direction. Thus, it could be used as an indication for the bending order of the joints. However, this could only be seen qualitatively, while the exact quantitative relation between the stiffness ratio and the slope of the PIP vs. DIP graph is inconclusive. The slopes that were predicted by using the relative stiffness do seem to correlate with the measured slopes, but there are clearly other factors affecting the response. It would require more samples to make any valid quantitative statements.

Regardless of this, one can certainly come to the conclusion that it is easy to modify joint stiffness by changing its thickness or width. However, the change in thickness will also affect the joint's strength, and the possibility of material failure under high strain situations, such as full flexion. By changing joint width, the stiffness is changed without an effect on strength, but also this option is effectively restricted by the actual width of the finger. Thus, a fine balance needs to be found between the two, if this type of flexure joint is used.

A joint thickness of 4 mm should be considered as a maximum for this joint geometry, because the finger with a 5 mm joint experienced a rapid failure after only a few full flexion experiments. The material failures in the areas of most stress concentration also imply that the joint geometry should be changed from a simple rectangular notch joint to e.g. elliptical, or adding large enough fillets in the corners, like Lobontiu instructs [60].

As mentioned in the results, the prototypes' actuated flexion phase differs notably from the non-actuated extension, with a hysteresis between the two. The main reason for this was that the fingers rose back from full flexion slightly slower than the servo motor released the tendon wire. Thus, the extension was not restricted as

much by the effects of friction and other tendon wire forces. This effect makes the response different from a real finger. However, as long as the fingers are made fast enough in their response, the hysteresis should become negligible, so that it would not have any significant effects on them.

The prototypes' joint angles slopes are also quite different from real. This is because in all, except in 02a, 03d, and 03e, there is a clear stiffness difference between the joints, which causes one of them to bend much faster. The same can be seen from the trajectory graphs. The real fingertip's path is round and resembles an equiangular curve to some degree, as described in literature [3]. Again, 02a, 03d and 03e had trajectories closest to this, because they had equal, or close to equal joints. These three configurations could thus be said to have the most *natural* response, while still being quite far from anthropomimetic.

Material

Although some of the material properties were given, the fact that the rubber's hardness was changed between prototype finger batches rendered them unusable for quantitative analysis, or simulation purposes. Thus, the material's effect was studied only qualitatively in the bending experiments, comparing the response of the soft finger to the harder ones.

The differences between the two types of material were easily observable. The harder fingers had a more sluggish response, and they required a lot more force for bending. They also started to show material failures much sooner than the soft one. These observations already show us that the soft version is superior of the two, although not perfect, and it should be used as a basis for further development.

The soft prototype exhibited similar soft tissue effects as the real finger, when it pressed on itself in full flexion. This was expressed as the waviness in the graphs. Furthermore, the harder prototypes did not compress much under load. This leads to the conclusion that the soft material would be better also in adapting to the shape of a grasped object, just like the natural skin compresses and envelops a firmly held item in the hand.

It should also be noted that the printing process affects the orientation of polymers in the structure. Thus, the directional strength of the material varies depending on the posture the object is printed in. Although the 3D-printing method may enable various optimal geometries, it may also cause non-optimal internal structures that could be prone to failure. This has to be considered in the future, because prostheses are subjected to constant cyclic loading during their normal use, and they should not fail or change their response radically during their predicted lifetime.

The stress relaxation, which was observed in the force measurements, is a normal phenomenon in these kinds of nonlinear systems. It affects the force that is essential for pulling the finger up. If it decreases too much, the finger's extension speed will decrease. Thus, it may be a major problem when a fast response is required after holding the finger in flexion for a longer time. Here, options are either making the extension phase actuated, or supporting the joint so that it does not lose its vigor in prolonged flexion.

Air pockets

The air pockets proved to have many positive effects on the finger that had them. The overall response and return to full extension were much faster than without them, the sideways rigidity was better, and the finger had a more anthropomorphic appearance.

They could, for example, provide a solution to the previously mentioned stress relaxation and sluggish response issues. The air inside the pockets will not have any mentionable creep or stress relaxation in itself, as long as the amount of entrapped gas stays the same. The air pocket structure will naturally try to return to the state of neutral pressure, which is in the initial position, defined by the manufactured structure.

The hysteresis effect was also clearly smaller with air pockets than with simple joints. The effect was minimized in configuration 03c, which had the air pocket behind the PIP joint, because it returned from flexion with the same speed as the servo motor released the wire. This can be seen as an advantage when considering the fingers' fast response, if the prosthetic hand is required to open quickly.

There are also problems with the structure. First, such structures increase the complexity of an already nonlinear mechanism, by including the interaction with air under pressure. Second, they restrict the finger's movement range. And third, they may be easily punctured, like a balloon, so that they lose some of their function. The last one could be solved by protecting the structure, or developing the material so that it is easy to repair. Also, the material could be developed so that it would have self-repair properties, like the materials described by Wietor and Sijbesma [68].

The air pockets should be investigated further, due to their potential benefits, to see if they could be utilized in practice. In their current form they have too many disadvantages that prevent their use in an actual prosthesis.

8.2 Realization of the concept

The prototype tests did not give a clear answer to whether the concept of MorphHand could work in practice. However, the response of the finger could be changed to the wanted direction by changing its morphological parameters. This shows that it may be possible to imitate the passive dynamic function of the human hand, if the structure is designed appropriately. This could perhaps be done to the degree that the device transfers some of the control to its morphology, and reduces the requirements for precise active control. Thus, the concept can still be considered realizable, until proven otherwise.

However, the results do imply that the prototype joint structure, used materials, and 3D-printing should be reconsidered, or significantly improved. The joint structure and the used material made the prototypes prone to failure, and their return from flexion slow. Also, it was uncertain, whether the material properties could be controlled well enough during the 3D-printing process to achieve an optimal level of stiffness and quality.

8.3 Future work

The ultimate goal in the development of MorphHand, is to produce a working prototype of a soft robotic hand prosthesis, and to evaluate its function to see whether the concept works or not. To have a complete design for a soft robotic prosthetic hand, many aspects would need to be considered. These include developing the structure further into a full hand, realizing its actuation, designing the control scheme, including sensors for feedback, and developing a HMI.

The next step is to develop the fingers further through simulations. The initial pseudo-rigid-body model that was derived in this thesis, could be used as a starting point. It should be expanded and completed, and validated against the measurement results. Then, it could be used as a design tool for producing the next generation of prototypes, and eventually a complete hand.

If the fingers are developed further, several other morphological parameters should be considered. Besides the ones that were tested in this thesis, there are e.g. the length and type of the flexural joint, and the attachment pin location relative to the joints' centerline, which affects the moment arm of the tendon wire. These should be considered in the future to find all the possible ways of modifying the response to the wanted direction.

As mentioned earlier, one of the main problems in the current finger implementation was the joint structure. A possible improvement for it is presented in Fig. 21. The flexure is made circular to gain better durability and stiffness. Also, the air pockets are added to the back to provide support and make the response faster.

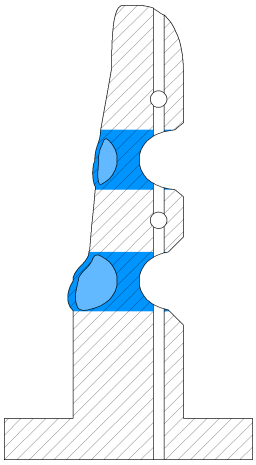

Figure 21: Proposal for a better joint structure. A circular flexure joint and the air pocket structure are combined to make the joint more durable and faster.

9 Conclusion

The goal of this thesis was to develop the concept of a soft robotic hand prosthesis, called MorphHand, and to explore the possibility of realizing it with the available methods. This was done by determining the design requirements and a working principle for the hand, based on a literature review, and manufacturing several two-joint prototype fingers, and testing them.

The tests confirmed that the analyzed parameters could be used for modifying the prototypes' response, and the experimental air pockets seemed promising for making the response faster, and the appearance more natural. However, the joint geometry and overall finger structure needs to be redesigned for durability. Also, problems with material durability, and structural quality of the 3D-printed prototypes, indicated that other materials and production methods should be considered.

Only one of the many possible ways of realizing the concept were described and tested for this thesis. The next steps will be developing a working finger structure, and then designing a complete hand, based on the defined requirements, and the lessons that were learned in this study.

In the end, the idea of using morphological computation and softness as key concepts seems promising for finding solutions to current problems in upper limb prosthetics. This thesis introduced MorphHand as an initial concept that gathered this idea into a single thought. If the hand is developed further, it will, as its name suggests, change along the way, and hopefully bring answers to these problems some day.

References

[1] J. L. Collinger, B. Wodlinger, J. E. Downey, W. Wang, E. C. Tyler-Kabara, D. J. Weber, A. J. C. McMorland, M. Velliste, M. L. Boninger, and A. B. Schwartz, "High-performance neuroprosthetic control by an individual with tetraplegia," *Lancet*, vol. 381, pp. 557–564, Feb. 2013.

[2] L. A. Jones and S. J. Lederman, *Human Hand Function*. New York, NY: Oxford University Press, 2006.

[3] R. Tubiana, J.-M. Thomine, and E. J. Mackin, *Examination of the Hand and Wrist*. New York, NY: Informa Healthcare, 2009.

[4] H. Gray, *Anatomy of the Human Body*. Philadelphia, PA: Lea & Febiger, 20th ed., 1918. Cited: 1.4.2014. Available: http://www.bartleby.com/107/.

[5] R. Dumas, L. Chèze, and J.-P. Verriest, "Adjustments to McConville et al. and Young et al. body segment inertial parameters," *Journal of Biomechanics*, vol. 40, no. 3, pp. 543–553, 2007.

[6] H. Liu, "Exploring human hand capabilities into embedded multifingered object manipulation," *IEEE Transactions on Industrial Informatics*, vol. 7, no. 3, pp. 389–398, 2011.

[7] R. F. Weir and J. W. Sensinger, "The design of artificial arms and hands for prosthetic applications," in *Biomedical Engineering and Design Handbook* (M. Kutz, ed.), vol. 2, ch. 20, pp. 537–598, McGraw Hill Professional, 2009.

[8] M. Barakat, J. Field, and J. Taylor, "The range of movement of the thumb," *HAND*, vol. 8, no. 2, pp. 179–182, 2013.

[9] J. Leijnse, P. Quesada, and C. Spoor, "Kinematic evaluation of the finger's interphalangeal joints coupling mechanism—variability, flexion–extension differences, triggers, locking swanneck deformities, anthropometric correlations," *Journal of Biomechanics*, vol. 43, no. 12, pp. 2381–2393, 2010.

[10] P. Hahn, H. Krimmer, A. Hradetzky, and U. Lanz, "Quantitative analysis of the linkage between the interphalangeal joints of the index finger," *Journal of Hand Surgery (British and European Volume)*, vol. 20B, no. 5, pp. 696–699, 1995.

[11] A. D. Deshpande, R. Balasubramanian, R. Lin, B. Dellon, and Y. Matsuoka, "Understanding variable moment arms for the index finger MCP joints through the ACT hand," in *Proc. 2nd IEEE RAS EMBS International Conference on Biomedical Robotics and Biomechatronics*, pp. 776–782, 2008.

[12] S. Takamuku, A. Fukuda, and K. Hosoda, "Repetitive grasping with anthropomorphic skin-covered hand enables robust haptic recognition," in *Proc. IEEE/RSJ International Conference on Intelligent Robots and Systems (IROS)*, pp. 3212–3217, 2008.

[13] E. D. Sherman, "A russian bioelectric-controlled prosthesis: Report of a research team from the rehabilitation institute of montreal," *Canadian Medical Association Journal*, vol. 91, pp. 1268–1270, Dec. 1964.

[14] A. B. Wilson Jr., "History of amputation surgery and prosthetics," in *Atlas of Limb Prosthetics: Surgical, Prosthetic, and Rehabilitation Principles*, ch. 1, Demos Medical Publishing, 1 ed., Feb. 1992. Cited: 1.4.2014. Available: http://www.oandplibrary.org/alp/.

[15] Y. Saito, A. Ogawa, H. Negoto, and K. Ohnishi, "Development of intelligent prosthetic hand adapted to age and body shape," in *Proc. IEEE 9th International Conference on Rehabilitation Robotics (ICRR)*, (Chicago, IL, USA), June 28 – July 1 2005.

[16] D. Benyon, P. Turner, and S. Turner, *Designing Interactive Systems – People, Activities, Contexts, Technologies*. Pearson Education, 2005.

[17] C. Connolly, "Prosthetic hands from Touch Bionics," *Industrial Robot: An International Journal*, vol. 35, no. 4, pp. 290–293, 2008.

[18] E. Biddiss, D. Beaton, and T. Chau, "Consumer design priorities for upper limb prosthetics," *Disability & Rehabilitation: Assistive Technology*, vol. 2, pp. 346–357, Jan. 2007.

[19] E. Biddiss and T. Chau, "Upper-limb prosthetics: critical factors in device abandonment," *American journal of physical medicine & rehabilitation*, vol. 86, pp. 977–987, Dec. 2007.

[20] J. Gibbard, "Open Hand Project website." Cited: 1.4.2014. Available: http://www.openhandproject.org/.

[21] K. Hagberg and R. Brånemark, "One hundred patients treated with osseointegrated transfemoral amputation prostheses – rehabilitation perspective," *Journal of Rehabilitation Research & Development*, vol. 46, no. 3, pp. 331–344, 2009.

[22] A. Bicchi, "Hands for dexterous manipulation and robust grasping: A difficult road toward simplicity," *IEEE Transactions on Robotics and Automation*, vol. 16, no. 6, pp. 652–662, 2000.

[23] R. R. Ma and A. M. Dollar, "On dexterity and dexterous manipulation," in *Proc. 15th International Conference on Advanced Robotics (ICAR)*, pp. 1–7, June 2011.

[24] B. Peerdeman, D. Boere, H. Witteveen, R. Huis in 't Veld, H. Hermens, S. Stramigioli, H. Rietman, P. Veltink, and S. Misra, "Myoelectric forearm prostheses: State of the art from a user-centered perspective," *Journal of Rehabilitation Research & Development*, vol. 48, no. 6, pp. 719–738, 2011.

[25] J. M. Burck, J. D. Bigelow, and S. D. Harshbarger, "Revolutionizing prosthetics: Systems engineering challenges and opportunities," *Johns Hopkins APL Technical Digest*, vol. 30, no. 3, pp. 186–197, 2011.

[26] M. S. Johannes, J. D. Bigelow, J. M. Burck, S. D. Harshbarger, M. V. Kozlowski, and T. Van Doren, "An overview of the developmental process for the Modular Prosthetic Limb," *Johns Hopkins APL Technical Digest*, vol. 30, no. 3, pp. 207–216, 2011.

[27] RSLSteeper, "RSLSteeper company website." Cited: 1.4.2014. Available: http://www.rslsteeper.com/.

[28] RSLSteeper, "beBionic product website." Cited: 1.4.2014. Available: http://www.bebionic.com/.

[29] RSLSteeper, *beBionic3 – technical information brochure*. Cited: 1.4.2014. Available: http://bebionic.com/.

[30] Touch Bionics, "Touch Bionics company website." Cited: 1.4.2014. Available: http://www.touchbionics.com/.

[31] Touch Bionics, *i-Limb Ultra Revolution – Clinician Manual*, Oct. 2013. Cited: 1.4.2014. Available: http://www.touchbionics.com/.

[32] Otto Bock Healthcare GmbH, "Otto Bock international, company website." Cited: 1.4.2014. Available: http://www.ottobock.com/.

[33] Otto Bock Healthcare GmbH, "Living with Michelangelo, product website." Cited: 1.4.2014. Available: http://www.living-with-michelangelo.com/.

[34] J. T. Belter and A. M. Dollar, "Performance characteristics of anthropomorphic prosthetic hands," in *Proc. IEEE International Conference on Rehabilitation Robotics (ICORR)*, pp. 921–927, Jan. 2011.

[35] J. T. Belter, J. L. Segil, A. M. Dollar, and R. F. Weir, "Mechanical design and performance specifications of anthropomorphic prosthetic hands: A review," *Journal of Rehabilitation Research & Development*, vol. 50, no. 5, pp. 599–618, 2013.

[36] E. A. Biddiss, "Upper limb prosthesis use and abandonment: A survey of the last 25 years," *Prosthetics and Orthotics International*, vol. 31, pp. 237–257, Sept. 2007.

[37] R. Deimel, C. Eppner, J. Álvarez-Ruiz, M. Maertens, and O. Brock, "Exploitation of environmental constraints in human and robotic grasping," in *Proc. International Symposium on Robotics Research (ISRR)*, Dec. 2013.

[38] H. Hauser, A. J. Ijspeert, R. M. Füchslin, R. Pfeifer, and W. Maass, "Towards a theoretical foundation for morphological computation with compliant bodies," *Biological Cybernetics*, vol. 105, no. 5-6, pp. 355–370, 2011.

[39] R. Pfeifer and J. C. Bongard, *How the Body Shapes the Way We Think: A New View of Intelligence*. The MIT Press, Nov. 2006.

[40] C. Paul, "Morphological computation: A basis for the analysis of morphology and control requirements," *Robotics and Autonomous Systems*, vol. 54, no. 8, pp. 619–630, 2006.

[41] R. Pfeifer, F. Iida, and G. Gómez, "Morphological computation for adaptive behavior and cognition," *International Congress Series*, vol. 1291, pp. 22–29, June 2006.

[42] R. Pfeifer, M. Lungarella, and F. Iida, "Self-organization, embodiment, and biologically inspired robotics," *Science*, vol. 318, no. 5853, pp. 1088–1093, 2007.

[43] T. McGeer, "Passive Dynamic Walking," *The International Journal of Robotics Research*, vol. 9, pp. 62–82, Apr. 1990.

[44] S. Kim, L. Cecilia, and B. Trimmer, "Soft robotics: a bioinspired evolution in robotics," *Trends in Biotechnology*, vol. 31, pp. 287–294, May 2013.

[45] C. Laschi, M. Cianchetti, B. Mazzolai, L. Margheri, M. Follador, and P. Dario, "Soft robot arm inspired by the octopus," *Advanced Robotics*, vol. 26, no. 7, pp. 709–727, 2012.

[46] R. Pfeifer, M. Lungarella, and F. Iida, "The challenges ahead for bio-inspired 'soft' robotics," *Communications of the ACM*, vol. 55, pp. 76–87, Nov. 2012.

[47] European Commission, 7th Framework Programme, "OCTOPUS Integrating Project website." Cited: 1.4.2014. Available: http://www.octopusproject.eu/.

[48] C. Majidi, R. F. Shepherd, R. K. Kramer, G. M. Whitesides, and R. J. Wood, "Influence of surface traction on soft robot undulation," *The International Journal of Robotics Research*, vol. 32, no. 13, pp. 1577–1584, 2013.

[49] F. Lotti, P. Tiezzi, G. Vassura, L. Biagiotti, G. Palli, and C. Melchiorri, "Development of UB Hand 3: Early results," in *Proc. IEEE International Conference on Robotics and Automation (ICRA)*, pp. 4488–4493, Apr. 2005.

[50] G. Palli, C. Melchiorri, G. Vassura, G. Berselli, S. Pirozzi, C. Natale, G. De Maria, and C. May, "Innovative technologies for the next generation of robotic hands," in *Advanced Bimanual Manipulation* (B. Siciliano, ed.), pp. 173–218, Berlin: Springer Berlin / Heidelberg, 2012.

[51] G. Borghesan, "Design of tendon-driven robotic fingers: Modeling and control issues," in *Proc. IEEE International Conference on Robotics and Automation (ICRA)*, pp. 793–798, 2010.

[52] F. Lotti and G. Vassura, "A novel approach to mechanical design of articulated fingers for robotic hands," in *Proc. IEEE/RSJ International Conference on Intelligent Robots and Systems*, vol. 2, pp. 1687–1692, 2002.

[53] A. M. Dollar and R. D. Howe, "The highly adaptive sdm hand: Design and performance evaluation," *International Journal of Robotics Research*, vol. 29, pp. 585–597, Apr. 2010.

[54] R. Deimel and O. Brock, "A compliant hand based on a novel pneumatic actuator," in *Proc. IEEE International Conference on Robotics and Automation (ICRA)*, pp. 2039–2045, 2013.

[55] M. C. Carrozza, G. Cappiello, G. Stellin, F. Zaccone, F. Vecchi, S. Micera, and P. Dario, "A cosmetic prosthetic hand with tendon driven under-actuated mechanism and compliant joints: Ongoing research and preliminary results," in *Proc. IEEE International Conference on Robotics and Automation (ICRA)*, (Barcelona, Spain), Apr. 2005.

[56] E. Ullmann, F. Cepolina, and M. Zoppi, "Upper limb prosthesis for developing countries," in *Proc. IEEE International Conference on Intelligent Manipulation and Grasping*, (Genova, Italy), 1–2 July 2004.

[57] J. Speich and M. Goldfarb, "A compliant-mechanism-based three degree-of-freedom manipulator for small-scale manipulation," *Robotica*, vol. 18, pp. 95–104, 1 2000.

[58] L. L. Howell, *Compliant Mechanisms*. New York, NY: John Wiley & Sons, 2001.

[59] L. L. Howell, S. P. Magleby, and B. M. Olsen, *Handbook of compliant mechanisms*. Chichester, West Sussex: John Wiley & Sons, Inc., 2013.

[60] N. Lobontiu, *Compliant Mechanisms: Design of Flexure Hinges*. CRC Press, 2003.

[61] H.-J. Su, "A pseudo-rigid-body 3R model for determining large deflection of cantilever beams subject to tip loads," *ASME Journal of Mechanisms and Robotics*, vol. 1, no. 2, pp. 021008:1–9, 2009.

[62] V. S. Ramachandran and W. Hirstein, "The perception of phantom limb. The D. O. Hebb lecture.," *Brain*, vol. 121, no. 9, pp. 1603–1630, 1998.

[63] M. Sekine, K. Sugimori, T. V. J. Tarvainen, and W. Yu, "Prototyping a parallel link arm driven by small pneumatic actuator for shoulder prostheses," in *Proc. IEEE International Conference on Robotics and Biomimetics (ROBIO)*, (Guangzhou, China), pp. 1391–1396, 10–14 Dec. 2012.

[64] T. V. J. Tarvainen, W. Yu, and J. Gonzalez, "Development of MorphHand: Design of an underactuated anthropomorphic rubber finger for a prosthetic hand using compliant joints," in *Proc. IEEE International Conference on Robotics and Biomimetics (ROBIO)*, (Guangzhou, China), pp. 142–147, 10–14 Dec. 2012.

[65] A. Buryanov and V. Kotiuk, "Proportions of hand segments," *International Journal of Morphology*, vol. 28, pp. 755–758, Sept. 2010. LILACS ID: 577181.

[66] Three Esu (SSS) Co. Ltd., "Company website." Cited: 1.4.2014. Available: http://www.3esu.com/.

[67] Z. Feng, Y. Yu, and W. Wang, "Modeling of large-deflection links for compliant mechanisms," *Frontiers of Mechanical Engineering in China*, vol. 5, no. 3, pp. 294–301, 2010.

[68] J.-L. Wietor and R. P. Sijbesma, "A self-healing elastomer," *Angewandte Chemie International Edition*, vol. 47, no. 43, pp. 8161–8163, 2008.